

FLEXIBLE WEARABLE THERMOELECTRIC GENERATOR WITH
VERTICALLY ALIGNED ARCHITECTURE OF PEDOT:PSS AND CARBON
NANOTUBE FILMS

MD. NAZIBUL HASAN

UNIVERSITI TEKNOLOGI MALAYSIA

FLEXIBLE WEARABLE THERMOELECTRIC GENERATOR WITH
VERTICALLY ALIGNED ARCHITECTURE OF PEDOT:PSS AND CARBON
NANOTUBE FILMS

MD. NAZIBUL HASAN

A thesis submitted in fulfilment of the
requirements for the award of the degree of
Doctor of Philosophy

School of Electrical Engineering
Faculty of Engineering
Universiti Teknologi Malaysia

JULY 2022

ACKNOWLEDGEMENT

My heartfelt gratitude goes to my supervisor and principal investigator, Assoc. Prof. Ir. Dr. Mohamed Sultan Mohamed Ali, for providing me with the opportunity to work in the “Micro & Nano Technology Research Group” at Universiti Teknologi Malaysia (UTM), JB, Malaysia. I would like to thank him for guiding me throughout my research journey. His knowledge, unending encouragement, and inspiration during my Ph.D. aided in my development as a researcher and as a person, for which I am eternally grateful.

I would like to express my appreciation to the following group members for their encouragement and support over the last few years: Dr. Marwan Nafea, Dr. Tariq Rehman, Dr. Krishna Veni Selvan, Dr. Noor Dzulaikha Daud, Dr. Fatimah Khairiah Abd Hamid, Yong Xian Ang, Aqilah Binti Abdul Tahrir, Farah Afiqa Mohd Ghazali, Mariatul Rawdhah Ahmad Fuaad, and Muhammad Izzudin Ahmad Asri. Everyone has been very supportive and encouraging throughout my research. My deep appreciation goes to Dr. Lukka Thuyavan Y. for assisting me with my fabrication work. Furthermore, I would like to thank all my research collaborators, including Dr. Kenichi Takahata (University of British Columbia), Dr. Asan G. A. Muthalif (Qatar University), Dr. Nafarizal Nayan (Universiti Tun Hussein Onn Malaysia), Dr. Marwan Nafea (University of Nottingham Malaysia), and Dr. Tanveer Saleh (IIUM).

In addition, I would like to take this opportunity to express my sincere thanks to all my friends: Sheikh Khairuzzaman, Sofiur Rahman, Dr. Rajesh, Namrata, Soni, Praveen, Dr. Debanjan, Debabrata, Ram Acharya, Saswati, Dr. Paromita, Pavan Chaganti, Wahid, Abdullah, Yusuf, Raihan, Mehdi, Shahed, Sajjad, and Emon for their endless moral support. I owe a massive debt of gratitude to all the people who have made my Ph.D. journey possible.

I would like to thank all my family members for their endless support and love. I certainly would not be the person I am today without the support and sacrifice of my beloved father, Mohammed Abdul Hamid, and mother, Nazia Hasan. They have supported me in every way possible over the years, and I cannot express how thankful I am and how much it means to me to have them as my parents. I would like to extend my thanks to my brother, Mohammed Nakibul Hasan, for his encouragement, love, and support. My special appreciation goes to all my family members for their love and support.

ABSTRACT

Energy harvesting has become pivotal for wearable electronics, which require a constant power supply. Recent research has paved the way for the development of a wide variety of self-powered devices that harvest energy from the human body. Thermoelectric generators (TEGs) facilitate maintenance-free sustainable energy transduction, making them an enticing and feasible option for harvesting energy. Notwithstanding, their energy conversion process suffers because of inadequate design and rigidity owing to the use of brittle and toxic inorganic material-based thermoelements, making them inappropriate for energy harvesting from the human body. To address the issues, flexible wearable TEGs have been developed by integrating flexible conducting polymer based thermoelements. Nonetheless, their performance suffered significantly due to the deficient TEG designs, where thermoelements were integrated into the lateral layout with cross-plane heat flow direction. The design and implementation of such lateral TEGs is challenging for harvesting energy from the human body, where the temperature gradient (ΔT) lies between the body heat and the ambient temperature. Thus, developing a vertical structured TEG with flexible thermoelements with high deformability is a requisite. In this thesis, novel wearable TEGs with vertically aligned architecture of thermoelements based on flexible organic poly(3,4-ethylenedioxythiophene): polystyrene sulfonate (PEDOT:PSS) and single-wall carbon nanotube (SWCNT) films were designed and fabricated. Finite element analysis was performed to analyze the heat dissipation through the thermoelements as well as to optimize their length for the highest ΔT and enhanced output performance. Thermoelements were prepared via solution-processing and drop-cast techniques, while the overall architectures of the TEGs were developed through low-cost 3D printing followed by a sacrificial molding technique. Flexible polydimethylsiloxane was used to develop TEG structures and encapsulation layers for all the thermoelements. The structures possess a high degree of flexibility and can sustain a maximum bending angle of 52 degrees without significantly changing their electrical parameters. In addition, this thesis examined the effects of acid-based post-treatments and polyethylenimine concentration on the performance of the thermoelectric properties of PEDOT:PSS and SWCNT films, respectively. As a proof of concept, a TEG was initially developed using five pairs of *p*-type PEDOT:PSS film and *n*-type aluminum wire-based thermoelements that produced an open-circuit voltage (V_{oc}) and output power density (P_d) of 1.46 mV and 1.5 nWcm⁻², respectively, at a ΔT of 11.27 °C from the wrist. Likewise, another TEG was composed of five pairs of *p*-type PEDOT:PSS and *n*-type SWCNT film-based thermoelements that generated a V_{oc} and P_d of 1.75 mV and 10.17 nWcm⁻², respectively, at a ΔT of 11.24 °C from the wrist. The proposed design approaches represent a significant step toward developing next-generation flexible organic TEG that could pave the way for self-powered wearable electronics in a sustainable way by utilizing the body heat.

ABSTRAK

Penjanaan tenaga telah menjadi element penting untuk peranti elektronik boleh pakai yang memerlukan bekalan kuasa yang berterusan. Penyelidikan baru-baru ini telah membuka jalan kepada pembangunan pelbagai jenis peranti berkuasa sendiri yang menjana tenaga daripada haba badan manusia. Penjana termoelektrik (TEGs) menyediakan transduksi tenaga mampan tanpa penyelenggaraan, menjadikannya pilihan yang menarik dan boleh laksana untuk menjana tenaga. Walau bagaimanapun, proses penukaran tenaga ini menghadapi masalah pada reka bentuk dan ketegaran yang terhad disebabkan penggunaan termoelemen berasaskan bahan tidak organik yang rapuh dan toksik, menjadikannya tidak sesuai untuk penggunaan penjanaan tenaga daripada tubuh manusia. Untuk mengatasi masalah ini, TEG dibangunkan dengan menggunakan polimer pengalir elektrik fleksibel. Namun begitu, prestasi TEG terjejas dengan ketara akibat kelemahan reka bentuk TEG, di mana termoelemen telah diintegrasikan ke dalam susun atur datar dengan arah aliran haba satah silang. Reka bentuk dan pelaksanaan TEG datar sangat mencabar, terutamanya untuk menjana tenaga daripada haba badan manusia, di mana perbezaan suhu (ΔT) terletak di antara suhu badan dan suhu persekitaran. Oleh itu, pembangunan peranti TEG menegak menggunakan termoelemen polimer pengalir yang fleksibel amat diperlukan. Dalam tesis ini, TEG boleh pakai novel yang dilengkapi dengan termoelemen dijajar menegak berdasarkan organik fleksibel poli(3,4-etilena-dioksitiofen):polistirena sulfonat (PEDOT:PSS) dan tiub nano karbon dinding tunggal (SWCNT) telah direka bentuk dan dihasilkan. Analisis unsur terhingga telah dilakukan untuk menganalisis pelepasan haba melalui termoelemen serta untuk mengoptimumkan panjang struktur termoelemen untuk mencapai ΔT dan prestasi keluaran yang baik. Termoelemen telah disediakan melalui pemprosesan larutan dan teknik drop-cast, manakala struktur keseluruhan TEGs dibangunkan melalui percetakan 3D kos rendah diikuti dengan teknik pengacuan sementara. Bahan polydimethylsiloxane yang fleksibel digunakan untuk membangunkan struktur TEG dan lapisan enkapsulasi untuk semua termoelemen. Struktur TEG mempunyai tahap fleksibiliti yang tinggi dan boleh mengekalkan sudut lentur maksimum 52 darjah tanpa mengubah parameter elektriknya dengan ketara. Di samping itu, tesis ini juga mengkaji kesan pasca rawatan berasaskan asid dan kepekatan bahan polietilenimin terhadap prestasi sifat filem termoelektrik PEDOT:PSS dan SWCNT. Sebagai bukti konsep, TEG pada mulanya dibangunkan menggunakan lima pasang filem PEDOT:PSS jenis-*p* dan termoelemen berasaskan wayar aluminium jenis-*n* yang menghasilkan voltan litar terbuka (V_{oc}) dan ketumpatan kuasa keluaran (P_d) masing-masing sebanyak 1.46 mV dan 1.5 nWcm⁻², pada ΔT 11.27 °C dari pergelangan tangan. Dengan cara yang sama, satu lagi TEG yang terdiri daripada lima pasang PEDOT:PSS jenis-*p* dan termoelemen berasaskan filem SWCNT jenis-*n* yang menghasilkan V_{oc} dan P_d masing-masing 1.75 mV dan 10.17 nWcm⁻², pada ΔT 11.24 °C dari pergelangan tangan. Pendekatan reka bentuk yang dicadangkan ini merupakan langkah penting ke arah membangunkan TEG organik fleksibel generasi akan datang bagi peranti elektronik boleh pakai berkuasa sendiri dengan cara yang mampan dengan menggunakan haba badan.

TABLE OF CONTENTS

	TITLE	PAGE
	DECLARATION	iii
	DEDICATION	v
	ACKNOWLEDGEMENT	v
	ABSTRACT	vi
	ABSTRAK	vii
	TABLE OF CONTENTS	viii
	LIST OF TABLES	xii
	LIST OF FIGURES	xiii
	LIST OF ABBREVIATIONS	xx
	LIST OF SYMBOLS	xxiii
CHAPTER 1	INTRODUCTION	1
1.1	Motivation	1
1.2	Problem Statements and Research Gaps	3
1.3	Research Objectives	6
1.4	Research Scopes	7
1.5	Research Significances	8
1.6	Thesis Outlines	9
CHAPTER 2	LITERATURE REVIEW	11
2.1	Introduction	11
2.2	Thermoelectric Energy Generation Mechanism	13
2.3	Classification of Thermoelectric Generator	15
2.3.1	Vertical-Structured TEG with a Cross-Plane Heat Flow Structure	17
2.3.2	Lateral-Structured TEG with a Cross-Plane Heat Flow Structure	19
2.3.3	Lateral-Structured TEG with an In-Plane Heat Flow Structure	20

2.4	State-of-the-art Thermoelectric Materials	22
2.4.1	Inorganic Thermoelectric Materials	24
2.4.1.1	Bismuth Telluride	24
2.4.1.2	Tin Selenide	26
2.4.1.3	Copper Selenide	28
2.4.1.4	Magnesium Antimonide	31
2.4.2	Organic Thermoelectric Materials	33
2.4.2.1	Conducting Polymers	37
2.4.2.1.1	Conjugated Polymers	37
2.4.2.1.2	Metal-Organic Coordination Polymers	43
2.4.2.2	Carbon Nanomaterials Composites	44
2.4.2.2.1	CNTs-based Polyaniline and PEDOT:PSS Composites	45
2.4.2.2.2	Graphene-based polyaniline and PEDOT:PSS composites	49
2.5	Challenges of Current Thermoelectric Generators and Plans for the Study	51
2.6	Chapter Summary	57
CHAPTER 3	RESEARCH METHODOLOGY	58
3.1	Introduction	58
3.2	Methodology	58
3.2.1	Phase I: TEG with Vertically Aligned PEDOT:PSS Thermoelements	61
3.2.2	Phase II : TEG with Vertically Aligned PEDOT:PSS and SWCNT Films-Based Thermoelements	61
3.2.3	Structural Design of TEG Prototypes	62
3.2.4	Finite Element Analysis	63
3.2.5	Experimental Setup and Characterization Techniques	65
3.3	Chapter Summary	68

CHAPTER 4	NOVEL STRUCTURAL DESIGN OF WEARABLE THERMOELECTRIC GENERATOR WITH VERTICALLY ALIGNED PEDOT:PSS THERMOELEMENTS	70
4.1	Introduction	70
4.2	Design Configuration of the Proposed TEG	71
4.3	Material Synthesis	73
4.4	Device Fabrication	74
4.5	Material Characterization Results	77
4.6	Characterization Results of the Fabricated TEG	78
	4.6.1 Demonstration of Energy Harvesting from the Human Body	81
4.7	Chapter Summary	83
CHAPTER 5	WEARABLE THERMOELECTRIC GENERATOR WITH VERTICALLY ALIGNED PEDOT:PSS AND SWCNT FILMS THERMOELEMENTS	85
5.1	Introduction	85
5.2	Design Configuration of the Proposed Flexible TEG	85
5.3	Material Synthesis	88
	5.3.1 Preparation of PEDOT:PSS Film	88
	5.3.2 Preparation of SWCNT Film	90
5.4	Device Fabrication	91
5.5	Material Characterization Results	93
5.6	Characterization Results of the Fabricated TEG	96
	5.6.1 Demonstration of Energy Harvesting from the Human Body	98
5.7	Performance Comparisons and Discussions	99
5.8	Chapter Summary	103
CHAPTER 6	CONCLUSION AND RECOMMENDATIONS	104
6.1	Conclusion	104
6.2	Research Contributions and Novelities	106
6.3	Future Works	107
REFERENCES		108

LIST OF TABLES

TABLE NO.	TITLE	PAGE
Table 1.1	Miniaturized energy harvesting techniques and their characteristics	4
Table 2.1	Summary of the best-performing inorganic thermoelectric materials and their properties at the specific temperature range	34
Table 2.2	Summary of the best-performing organic thermoelectric materials and their properties at the near-room temperature	52
Table 3.1	Material properties used during the simulation	64
Table 5.1	Performance comparisons between this research and previously published wearable thermoelectric generators with PEDOT:PSS thermoelements	101

LIST OF FIGURES

FIGURE NO.	TITLE	PAGE
Figure 1.1	A schematic illustration of various wearable sensors capable of measuring physiological signals in the human body along with their power requirements	2
Figure 2.1	Graphical overview of the energy harvesters along with their major application areas	12
Figure 2.2	Schematic diagram showing a TEG with thermoelement pairs and its equivalent circuit model with electrical resistance networks	14
Figure 2.3	Schematic diagram of TEG classification	16
Figure 2.4	Schematic diagram showing (a) vertical-structured TEG with a cross-plane heat flow structure. (b) TEG-powered ECG sensor system. Reprinted with permission from Ref. [44] Copyright (2020), American chemical society. (c) TEG prototype and (d) its integration on the glucose sensor system. Reprinted with permission from Ref. [62] Copyright (2020), Elsevier. (e) TEG-powered multifunctional e-skin. Reprinted with permission from Ref. [63] Copyright (2020), Elsevier. (f) TEG-powered wearable multisensory bracelet. Reprinted with permission from Ref. [64] Copyright (2020), Elsevier	18
Figure 2.5	Schematic diagram showing (a) lateral-structured TEG with a cross-plane heat flow structure. (b) Schematic diagram of a SiNW-TEG fabricated on silicon substrate. Reproduced with permission. [66] Copyright 2018, Taylor & Francis Group. silicon integrated circuit-TEG prototype. (c) Schematic diagram of thermoelement pair composed of <i>n</i> - and <i>p</i> -type blades attached by tungsten (W) plugs, (d) SEM cross-section depicting a single four-blade (top of each blade is 80 nm wide) group with W contacts, heat exchange fins, and a serpentine heater. Reproduced with permission [36]. Copyright 2019, Nature Publishing Group	19
Figure 2.6	Schematic diagram showing (a) lateral-structured TEG with a cross-plane heat flow structure. (b) Amalgamation of TEG in FiNFET. Reproduced with permission.[67] Copyright 2013, IEEE. silicon integrated circuit-TEG prototype. (c) All-fabric wearable TEG. Reproduced with permission. [68] Copyright 2019, Wiley-VCH. (d) Wearable TEG. Reproduced with permission [69]. Copyright 2017, Elsevier. Flexible TEG in a plasma-treated	

- plastic substrate. Reproduced with permission.[70] Copyright 2016, Elsevier. (f) wearable TEG with PEDOT:PSS composite film. Reproduced with permission [71]. Copyright 2022, Elsevier 21
- Figure 2.7 Schematic diagram of thermoelectric material classification 23
- Figure 2.8 (a) Crystal structure of Bi_2Te_3 . Reprinted with permission from Ref. [77] Copyright (2019), Nature publishing group. (b) HAADF-STEM image of ND/ $\text{Bi}_{0.5}\text{Sb}_{1.5}\text{Te}_3$ composite and its (c) point-defect zone. Reprinted with permission from Ref. [82] Copyright (2019), Elsevier. (d) HAADF-STEM image of $\text{Bi}_{0.5}\text{Sb}_{1.5}\text{Te}_3$ sample. Reprinted with permission from Ref. [84] Copyright (2017), Elsevier. (e) Low resolution and (f) high resolution TEM images of BiSbTe matrix. Reprinted with permission from Ref. [85] Copyright (2017), Elsevier. (g) SEM images of Bi_2Te_3 nanotubes. Reprinted with permission from Ref. [86] Copyright (2014), RSC 25
- Figure 2.9 (a) Crystal structure of α -phase SnSe and (b) β -phase SnSe. Reprinted with permission from Ref. [88] Copyright (2018), Elsevier. (c) Schematic figure showing the process of doped SnSe/ CNT composite. Reprinted with permission from Ref. [92] Copyright (2018), Elsevier. (d) Schematic diagram showing the material synthesis process. SEM image of the synthesized flower-like $\text{Sn}_{0.948}\text{Cd}_{0.023}\text{Se}$ microplates. Reprinted with permission from Ref. [93] Copyright (2019), Wiley-VCH 27
- Figure 2.10 (a) Crystal structure of α -phase Cu_2Se . Reprinted with permission from Ref. [97] Copyright (2015), Elsevier. (b) SEM image of nanostructured Cu_2Se . (c) Schematics diagram illustrating the scattering process of phonons. Reprinted with permission from Ref. [98] Copyright (2015), Elsevier. (d) HRTEM image of nanostructured Cu_2Se showing distribution of fine nanocrystallites. Reprinted with permission from Ref. [99] Copyright (2015), Elsevier. (e) A schematic diagram provides a visual representation of eutectic transformation synthesis. The energy filtering effect and phonon scattering have a significant impact on the increased performance of carbon/boron-nanoparticles based- Cu_2Se . Performance comparison between the average figure-of-merit and the design figure-of-merit of carbon/boron α -nanoparticles based- Cu_2Se . (f) TEM image indicates the grain boundary region of the carbon/boron-nanoparticles based- Cu_2Se . Reprinted with permission from Ref. [101] Copyright (2019), Wiley-VCH. (g) SEM image of graphene nanoplates-based Cu_2Se . (h) Schematic diagram of the phase of nucleation contributing to tiny grains and its effect

- on τ . Reprinted with permission from Ref. [103] Copyright (2018), Elsevier 30
- Figure 2.11 (a) Crystal structure of Mg_3Sb_2 . Reprinted with permission from Ref. [107]. Copyright (2020), Elsevier. (b) SEM image of the cross-sectional surface of the $\text{Mg}_{2.69}\text{Li}_{0.01}\text{Cd}_{0.5}\text{Sb}_2$. Reprinted with permission from Ref. [110] Copyright (2020), American Chemical Society. (c) TEM image shows the microstructure morphology of $\text{Mg}_{2.9}\text{Y}_{0.1}\text{Sb}_{1.5}\text{Bi}_{0.5}$. Reprinted with permission from Ref. [112] Copyright (2019), Elsevier. (d) Low-magnification TEM image depicting $\text{Mg}_{3.15}\text{Mn}_{0.05}\text{Sb}_{1.5}\text{Bi}_{0.49}\text{Te}_{0.01}$ micrograins. Reprinted with permission from Ref. [113] Copyright (2018), Elsevier 32
- Figure 2.12 (a) Chemical structures of a few conjugated polymers in their undoped state. Polyaniline nanostructures with different acid-based dopants. (b) - naphthalene sulfonic acid. Reprinted with permission from Ref. [130] Copyright (2010), Elsevier. (c) Sulfosalicylic acid. Reprinted with permission from Ref. [131] Copyright (2014), Wiley-VCH. (d) *p*-toluenesulfonic acid. Reprinted with permission from Ref. [132] Copyright (2014), Elsevier 39
- Figure 2.13 (a) SEM images of PEDOT:PSS films with (left side) and without DMSO treatment (right side). Reprinted with permission from Ref. [136] Copyright (2021), Elsevier. (b) Schematic diagram illustrating the formation of PEDOT:PSS films with over-coating and dedoping techniques. Reprinted with permission from Ref. [139] Copyright (2014), The Royal Society of Chemistry. (c) Schematic diagram illustrating the formation of PEDOT:PSS films with doping and dedoping process. Reprinted with permission from Ref. [140] Copyright (2014), The Royal Society of Chemistry. (d) Schematic diagram illustrating the mechanism and fabrication process of thermoelectric properties enhancement of PEDOT:PSS via sequential treatment. Reprinted with permission from Ref. [74] Copyright (2018), Wiley-VCH. (e) Schematic diagram showing the PEDOT:PSS chains after TFA - treatment. Reprinted with permission from Ref. [142] Copyright (2019), Wiley-VCH 41
- Figure 2.14 (a) Microstructure morphology displaying a fiber-like structure of polyaniline/pyrrole/SWCNT composite (left side). Schematic diagram displaying the formation of the composites (right side). Reprinted with permission from Ref. [153] Copyright (2019), Elsevier. (b) Schematic diagram showing the formation of SWCNT/polyaniline composites by dedoping process. Reprinted with

	permission from Ref. [154] Copyright (2019), Elsevier. (c) Schematic diagram depicting the formation of CSA doped polyaniline and SWCNT/polyaniline composites via in situ polymerization technique. Reprinted with permission from Ref. [156] Copyright (2021), Elsevier. (d) Microstructure formation of A-CNT/ polyaniline composites (left side) and its power factor (right side). Reprinted with permission from Ref. [157] Copyright (2019), Elsevier. (e) Schematic diagram showing sequential dedoping-redoping treatment of SWCNTs/polyaniline and (f) its thermoelectric properties. Reprinted with permission from Ref. [158] Copyright (2021), American Chemical Society	46
Figure 2.15	(a) Dedoping mechanism of PEDOT:PSS/SWCNT film via NaOH treatment and (b) its effect on σ and S . Reprinted with permission from Ref. [159] Copyright (2019), Elsevier. (c) Schematic representation of the carrier energy filtering effect between SWCNTs and PEDOT:PSS interfaces. Reprinted with permission from Ref. [160] Copyright (2019), American Chemical Society. (d) Schematic illustration showing the formation of PEDOT:PSS/SWCNT composite films with ionic liquid. Reprinted with permission from Ref. [161] Copyright (2021), American Chemical Society. (e) Schematic illustration showing the layer-by-layer deposition process. Reprinted with permission from Ref. [162] Copyright (2016), Wiley-VCH	48
Figure 2.16	(a) Microstructure of polyaniline/3D-tubular graphene composites. (b) The synthesis process for the composites is depicted schematically. Reprinted with permission from Ref. [170] Copyright (2017), Elsevier. (c) Schematic diagram illustrating semi-interpenetrating networks formed by chemically bonded <i>p</i> -phenylenediamine-modified graphene and linear polyaniline. Reprinted with permission from Ref. [171] Copyright (2018), American Chemical Society. (d) Schematic diagram illustrating the formation of PEDOT:PSS/GQDs composites. Reprinted with permission from Ref. [173] Copyright (2018), Nature	50
Figure 3.1	Flowchart depicting the research methodology of the study	59
Figure 3.2	PDMS mold design for (a) first prototype and (b) second prototype	62
Figure 3.3	Mesh for PEDOT:PSS film, aluminum wire, and SWCNT film	65
Figure 3.4	(a) Schematic representation and (b) actual experimental setups for the fabricated wearable thermoelectric generator	66
Figure 3.5	Schematic diagram of general experimental setup	67

Figure 4.1	(a) Structural design of the wearable thermoelectric generator. (b) Graphical representation of wrist-worn thermoelectric generator	71
Figure 4.2	Finite element analysis results of the thermoelements. (a) Temperature distribution through PEDOT:PSS film and aluminum wire at a fixed temperature condition. (b) Temperature gradient as a function of the length of PEDOT:PSS and aluminum wire	73
Figure 4.3	(a) Image of the prepared HNO ₃ -treated PEDOT:PSS thin film. (b) PEDOT:PSS thin film showing flexibility. (c) SEM image of the prepared PEDOT:PSS thin film	74
Figure 4.4	Schematic illustrations of the fabrication process of the wearable thermoelectric generator incorporated with vertically aligned thermoelements	75
Figure 4.5	Fabrication results. (a) Image of the developed PDMS structure. (b) Side view of the wearable thermoelectric generator after the integration of vertically aligned PEDOT:PSS thin film and aluminum wire-based thermoelements. (c) Photograph of the wearable thermoelectric generator after being integrated into a wearable band	76
Figure 4.6	(a) Experimental setup used for PEDOT:PSS thin film characterization. (b) Seebeck coefficient value for the PEDOT:PSS thin film via slope technique	77
Figure 4.7	(a) Open-circuit voltage of the fabricated thermoelectric generator at different temperature gradient. (b) Resistance of the each thermoelements and the entire thermoelectric generator	79
Figure 4.8	(a) Output power of the thermoelectric generator as a function of load and temperature gradient. (b) Maximum output power and areal power density of the fabricated thermoelectric generator at matched load resistance as a function of temperature gradient	80
Figure 4.9	(a) Fabricated wearable thermoelectric generator showing flexibility. (b) Demonstration of the wearable thermoelectric generator on the wrist. (c) Infrared image showing the heat distribution of the wrist and the wearable thermoelectric generator	82
Figure 4.10	(a) Open-circuit voltage and (b) power generation of the wearable thermoelectric generator from the human wrist	83

Figure 5.1	Flexible wearable TEG for harvesting energy from the human body. (a) Schematic design illustration of the flexible wearable TEG and (b) its interface with the wrist. (c) Dimensions of the each thermoelements and overall surface area of the TEG. Finite element analysis results of the thermoelements. (d) Temperature gradient as a function of the length of PEDOT:PSS and SWCNT films. (e) Simulation results of the temperature gradient across the length of the thermoelements. (f) Temperature distribution along the arc length of the optimally sized thermoelements	86
Figure 5.2	(a) Photograph of a piece of DMSO-mixed PEDOT:PSS thin film prepared showing its (b) high level of flexibility. Images captured with a scanning electron microscope of the synthesized DMSO-mixed PEDOT:PSS film (c) with HNO ₃ and (d) with H ₂ SO ₄ post-treatment. (e) Photograph of a piece of PEI/SWCNT thin film demonstrating its (f) high level of flexibility. Images captured with field-emission scanning electron microscopy of (g) synthesized pure SWCNT film and (h) PEI-brushed SWCNT film	89
Figure 5.3	(a) Photograph of a piece of DMSO-mixed PEDOT:PSS thin film prepared showing its (b) high level of flexibility. Images captured with a scanning electron microscope of the synthesized DMSO-mixed PEDOT:PSS film (c) with HNO ₃ and (d) with H ₂ SO ₄ post-treatment. (e) Photograph of a piece of PEI/SWCNT thin film demonstrating its (f) high level of flexibility. Images captured with field-emission scanning electron microscopy of (g) synthesized pure SWCNT film and (h) PEI-brushed SWCNT film	92
Figure 5.4	Setups for the PEDOT:PSS and SWCNT films. (a) Schematic representation of thermoelement to be measured and (b) actual setup of the measurement. (c) Dimensions of the PEDOT:PSS and SWCNT films	93
Figure 5.5	Slope technique for determining the Seebeck coefficient values. (a) Thermoelectric voltage generated by a PEDOT:PSS film as a function of temperature gradient. (b) Thermoelectric voltage generated by SWCNT films as a function of temperature gradient	94
Figure 5.6	Thermoelectric properties of the synthesized PEDOT:PSS and SWCNT films. (a) Electrical conductivity, (b) Seebeck coefficient, and (c) power factor of PEDOT:PSS films after DMSO, HNO ₃ and H ₂ SO ₄ treatments. Effects of PEI concentration on (d) electrical conductivity, (e) Seebeck coefficient, and (f) power factor of SWCNT films	95
Figure 5.7	Characterization results of the fabricated flexible wearable TEG. (a) V_{oc} as a function of ΔT and thermoelement pairs. (b) Output power as a function of load and ΔT . (c)	

Maximum output power and (d) areal power density at matched load while varying the ΔT

97

Figure 5.8 Demonstration of energy harvesting using the developed TEG attached to the wrist. (a) Infrared thermal image of the TEG along with the wrist. (b) A photo showing the developed flexible TEG mounted on the wrist and voltage generation from it. (c) V_{oc} and (d) power generation by the TEG from the wrist. (e) Flexibility and (f) resistance deviation as a function of bending angle of the TEG

99

LIST OF ABBREVIATIONS

ABS	-	Acrylonitrile butadiene styrene
Ag	-	Silver
BaTiO ₃	-	Barium titanate
BHS	-	Benzenehexaselenolate
BHT	-	Butylated hydroxytoluene
Bi	-	Bismuth
Bi ₂ Te ₃	-	Bismuth telluride
BSA	-	Benzenesulfonic acid
Br	-	Boron
BZT	-	Barium Zirconate Titanate
Cd	-	Cadmium
CMOS	-	Complementary metal-oxide-semiconductor
CNTs	-	Carbon nanotubes
CSA	-	Camphorsulfonic acid
Cu	-	Copper
Cu ₂ Se	-	Copper selenide
DMSO	-	Dimethyl sulfoxide
DWCNT	-	Double-walled carbon nanotubes
ECG	-	Electrocardiogram
EDOT	-	3,4-ethylenedioxythiophene
EG	-	Ethylene glycol
FEA	-	Finite element analysis
FESEM	-	Field-emission scanning electron microscope
FinFET	-	Fin field-effect transistor
E-skin	-	Electronic skin
Ge	-	Germanium
GQDs	-	Graphene quantum dots
HAADF	-	High-angle annular dark-field
HCl	-	Hydrochloric acid
HNO ₃	-	Nitric acid

H ₂ SO ₄	-	Sulphuric acid
La ₂ O ₃	-	Lanthanum oxide
Li	-	Lithium
LSM	-	Liquid state manipulation
Mg	-	Magnesium
Mg ₃ Sb ₂	-	Magnesium antimonide
Mn	-	Manganese
Mn ₂ O ₃	-	Manganese(III) oxide
MWCNT	-	Multi-walled carbon nanotubes
Na	-	Sodium
NaCl	-	Sodium chloride
NaOH	-	Sodium hydroxide
ND	-	Nano-diamond
<i>p</i> -TSA	-	<i>p</i> -toluenesulfonic acid
Pb	-	Lead
PDMS	-	Polydimethylsiloxane
PEDOT	-	Poly (3,4-ethylenedioxythiophene)
PEDOT:PSS	-	Poly(3,4-ethylenedioxythiophene): polystyrene sulfonate
PEGs	-	Piezoelectric generators
PEI	-	Polyethylenimine
PSS	-	Polystyrene sulfonate
PSSH	-	Polystyrene sulfonate acid
PVDF	-	Polyvinylidene fluoride
Se	-	Selenide
SEM	-	Scanning electron microscope
SiNW	-	Silicon nanowire
STEM	-	Scanning transmission electron microscopy
SnSe	-	Tin Selenide
Sn	-	Tin
SPS	-	Spark plasma sintering
SSA	-	Sulfosalicylic acid
SWCNT	-	Single-wall carbon nanotube
Te	-	Tellurium

TEM	-	Transmission electron microscopy
TEGs	-	Thermoelectric generators
TEG	-	Thermoelectric generator
TENGs	-	Triboelectric nanogenerators
TFA	-	Trifluoroacetic acid
TSA	-	Trichostatin A
Y ₂ O ₃	-	Yttrium oxide
Zn	-	Zinc

LIST OF SYMBOLS

D	-	Dimensional
ΔT	-	Temperature gradient
	-	Electrical conductivity
n	-	Electrical conductivity of n -type thermoelement
p	-	Electrical conductivity of p -type thermoelement
e	-	Thermal conductivity due to electron
lat	-	Lattice thermal conductivity
t	-	Thermal conductivity
μ	-	Mobility of charge carriers
	-	Electrical resistivity
A	-	Thermoelement area
A_n	-	Area of n -type thermoelement
A_p	-	Area of p -type thermoelement
A_{TEG}	-	Total surface area of TEG
E_g	-	Bandgap energy
i	-	Electrical current
l	-	Length of a thermoelement
l_n	-	Length of n -type thermoelement
L	-	Lorenz number
l_p	-	Length of p -type thermoelement
n	-	Carrier concentration
N_{TE}	-	Number of p -and n -type thermoelement pairs
P_d	-	Power density
P_{max}	-	Maximum output power
P_o	-	Output power
Q	-	Heat transfer rate
q	-	Heat flux
R_c	-	Contact resistance
R_i	-	Internal resistance of thermoelements
R_{in}	-	Internal resistance of a TEG

R_l	-	Load resistance
S	-	Seebeck coefficient
S_{pn}	-	Seebeck coefficient between p -and n -type thermoelements
S_n	-	Seebeck coefficient of n -type thermoelement
S_p	-	Seebeck coefficient of p -type thermoelement
T	-	Operating temperature
T_c	-	Cold side temperature
T_h	-	Hot side temperature
V_{oc}	-	Open-circuit voltage
ZT	-	Dimensionless figure of merit

CHAPTER 1

INTRODUCTION

1.1 Motivation

Over the last few decades, major transitions in the microelectronic industry, including size reduction, low-power consumption, and intensifying functionality, have triggered the development of various electronic devices. In particular, wearable technologies and biomedical devices have attracted considerable interest in recent times owing to their broad applications in medical diagnostics, precision therapy, and real-time health tracking, such as heart rate and blood pressure monitoring [1-3]. In addition, the convergence of these devices with the Internet-of-Things has recently gained significant attention. The convergence allows the devices to be equipped with wireless connectivity that directly transmits data into a cloud-based diagnostic server for further analysis and clinical evaluation. In particular, these devices could monitor an activity continuously using real-time data, thus having the potential to greatly minimize travel costs and the time needed for long-term monitoring [4, 5]. As an example, a cardiovascular disorder called arrhythmia prevents the heart from pumping enough oxygenated blood into and deoxygenated blood away from peripheral tissues, resulting in permanent damage to brain cells, congestive heart failure, and stroke [6, 7]. Continuous long-term monitoring of the heart is therefore essential for the prevention of this disease.

Self-powered devices facilitate the continuous monitoring of real-time data over a longer period of time; thus, power consumption is a crucial aspect. Figure 1.1 shows several vital sensors whose power consumption is within the range of nW to mW [8-12]. The power requirements of most of these devices are provided by conventional lithium-ion batteries due to their high P_d and longevity. In addition to these, the latest batteries, such as metal-sulfur [13], sodium [14], and environmental

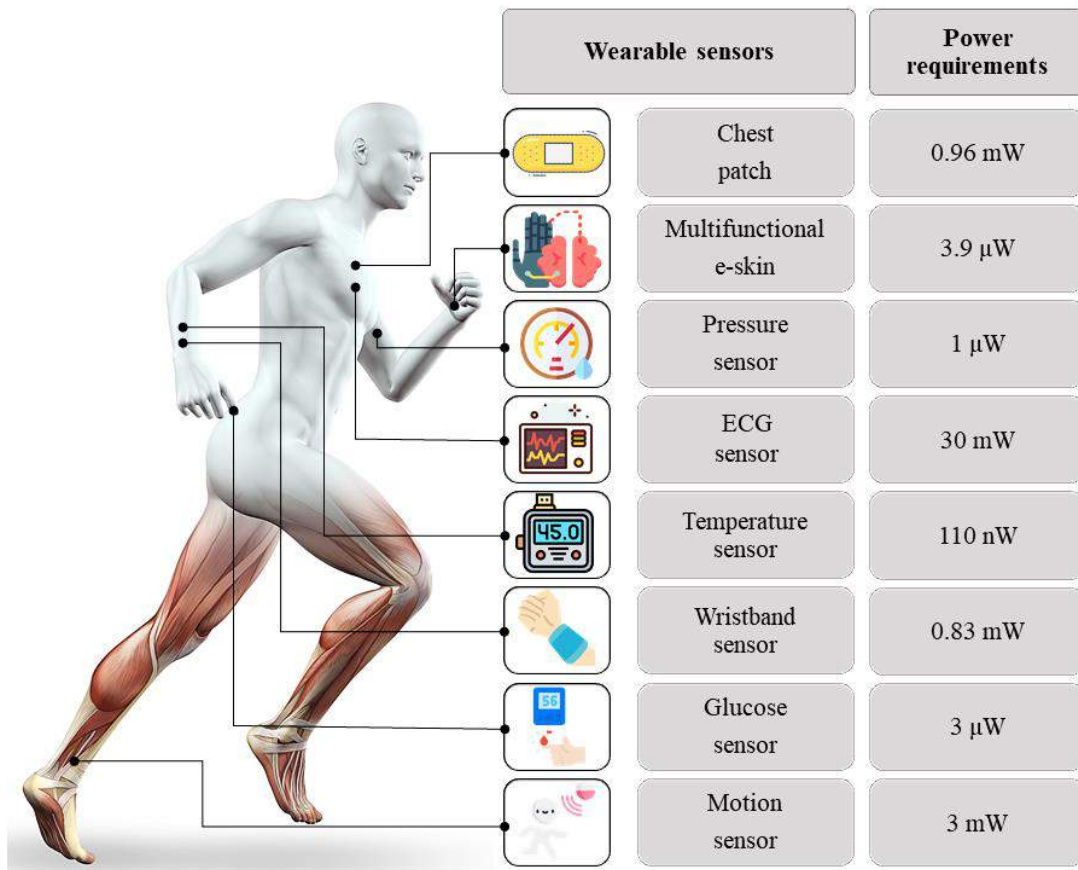


Figure 1.1 A schematic illustration of various wearable sensors capable of measuring physiological signals in the human body along with their power requirements

friendly aqueous zinc batteries [15], which are flexible and wearable, have also been developed as power sources for various electronic devices. However, most of these batteries either need to be replaced or recharged periodically. Although the present-day high-capacity batteries are compact and lightweight, and can provide sufficient energy to these devices, nonetheless, their versatility has been substantially reduced due to their restricted battery size and lifespan. Consequently, continuous power supply has become a major constraint for these devices.

On the other hand, promising alternative approaches have been developed to transform small-scale ambient energies, such as heat, mechanical vibration, or movement, into electrical power by means of ubiquitous miniaturized renewable energy transducers, including piezoelectric generators (PEGs) [16-18], triboelectric

nanogenerators (TENGs) [19-21], and thermoelectric generators (TEGs) [22-24]. These transducers can either be utilized as an extension to batteries to provide a long-term power supply or as a sole power supply. Table 1.1 presents a summary and comparison of the performance of these energy harvesting techniques. All these techniques have offered numerous advantages features, and are thus employed in several applications. Despite this progress, the use of such energy harvesters in a variety of wearable technologies is still in its infancy, with numerous challenges ahead. For example, PEG is capable of transmitting power across a wide range of frequencies and amplitudes without generating heat during operation. However, the majority of high-performance piezoelectric materials (such as lead zirconate titanate and barium zirconate titanate) are brittle and toxic, limiting their use in wearable flexible devices. TENG, on the other hand, offers high output performance as well as great flexibility; however, integration with wearable devices necessitates device miniaturization. Moreover, the performance of TENG devices is limited by the scarcity of triboelectric materials used in their fabrication as well as by the high abrasion rate of the materials.

Alternatively, among the energy transducers, TEGs are envisaged as a type of heat energy transducer with unique traits that make them attractive for a variety of applications. More precisely, since heat is one of the most widely accessible sources of energy that is also produced by the human body, TEGs hold advantages for harvesting energy and powering wearable technologies and biomedical devices without requiring any maintenance. Moreover, a wide range of non-poisonous highly flexible thermoelectric materials is also available. The efforts to reduce or eliminate the reliance on batteries through the use of body-worn TEG may thus intensify in tandem with the advancement of technologies to improve the continuous functionality of such devices.

1.2 Problem Statements and Research Gaps

Harvesting energy from the human body with TEGs has encountered several difficulties, as their temperature gradient (ΔT) is low due to the low human body heat.

Table 1.1 Miniaturized energy harvesting techniques and their characteristics

Energy Harvesting Techniques	Working Mechanism	Energy sources	Advantageous	Disadvantageous
PEG [25-29]	Piezoelectric effect	Cardiac motion, saliva swallowing, carotid artery pulse, and vibration of the pacemaker	No heating impact when the device is in use, fast response, tinier size, compact structure, highly sensitive to applied strain, provides reasonable P_d , and has greater life cycle	Highly efficient piezoelectric materials are poisonous, brittle, and expensive; need high-thermal processing for the integration of piezo materials and less efficient at low-frequency
TENG [30-33]	Electrostatic induction and contact electrification	Cardiac motion, blood flow, human body motion, finger friction, and wind blows	It can be utilized at high frequency, provides decent P_d , has a high energy conversion rate, easily scalable, highly bendable, lightweight, and maintenance-free	Its polarity and induced charge are highly dependent on the materials, and triboelectric materials have a high abrasion rate
TEG [34-36]	Seebeck effect	Human body heat and solar radiation	It has no moving parts, lightweight, high reliability, easily scalable, easy to integrate with other devices, and requires low-cost fabrication techniques	It requires a thermal gradient and is less efficient at converting energy

To overcome this challenge, simultaneous advances in the design of thermoelement, heat flow direction, as well as thermoelectric materials are required [37, 38]. For harvesting energy from the human body, both vertical and lateral-structured wearable TEGs have been widely used. Thermoelements are positioned perpendicularly to the substrate in vertically structured TEGs, and the heat flows in a cross-plane direction. In contrast, thermoelements in lateral structures are placed parallel to the substrate with a lateral heat flow direction [37]. A limited number of papers have been reported on vertically structured TEGs with all inorganic thermoelectric materials, notably with bismuth telluride (Bi_2Te_3) [38, 39] and antimony-telluride [40, 41] for energy harvesting from the human body because of their high performance at near-room temperatures. Regrettably, the practical applications of these flexible TEGs with such thermoelements for harvesting energy from the human body have been impeded on account of the toxicity and hazardous nature of the materials used. Moreover, inorganic materials are very expensive and require a dedicated fabrication process to achieve the desired thermoelement shape for incorporation into a flexible structure, which is a vital requirement for wearable devices.

To address these issues, a viable contemporary approach is to incorporate organic materials as thermoelements into TEGs, which could alleviate these problems for low-temperature thermoelectric applications. Organic materials exhibit high flexibility and an imponderous nature, and they require easy solutions and fabrication processes to make them into a versatile form. Among various organic materials, conducting polymers, notably poly(3,4-ethylenedioxythiophene):polystyrene sulfonate (PEDOT:PSS), and carbon nanomaterial composites, notably, single-wall carbon nanotube (SWCNT), have shown great potential for thermoelectric applications due to their high tenable electrical conductivity () and Seebeck coefficient (S) values, and stable chemical properties [42]. Moreover, the simple doping process enables them to tune the properties of the material to n - and p -type with a high thermoelectric property value. Realizing these benefits, a limited number of studies have synthesized and utilized PEDOT:PSS film as a p -type thermoelement and fabricated flexible TEGs for harvesting energy from the human body, which is typically laterally structured with an in-plan heat flow [43].

Even though the preceding studies showed significant flexibility in terms of the TEG structure and appreciable output performance with organic materials, such as PEDOT:PSS and SWCNT, their performance suffered significantly due to the low ΔT because of the laterally placed thermoelements in the TEGs. In addition, the TEGs were designed in such a way that they were not flexible enough and arduous to incorporate into the human body. Furthermore, none of the studies optimized the length of the PEDOT:PSS and SWCNT thin film thermoelements, which was required to achieve a high P_o , P_{max} , and an elevated P_d . As a result, it is desirable to fabricate a flexible wearable TEG with optimized vertically aligned thermoelements to ensure better heat transfer capability that can fit well with the human body.

1.3 Research Objectives

Wearable TEGs combined with thermoelements made of flexible organic materials have the potential to harvest energy from the human body. They have numerous advantages, including instantaneous energy conversion without having any moving parts, high reliability and stability, and inexpensive fabrication costs. Herein, the purpose of this research is to develop TEGs with vertically aligned organic thermoelements based on PEDOT:PSS and SWCNT thin films and characterize their performances. This design concept intends to maximize heat dissipation through thermoelements, enhance ΔT and output performance, while also alleviating the issue of wearability. To be more specific, the following are the research objectives to be achieved through this study:

- (a) To design and synthesize PEDOT: PSS and SWCNT thin films to achieve optimal length with highest ΔT for thermoelectric energy harvesting from the human body.
- (b) To design and fabricate a novel flexible wearable TEG comprised of vertically aligned architecture of PEDOT:PSS thin film thermoelements.

- (c) To design and fabricate a novel flexible wearable TEG comprised of vertically aligned architecture of PEDOT:PSS and SWCNT thin film thermoelements.
- (d) To experimentally characterize the performance of synthesized PEDOT:PSS and SWCNT thin films and the fabricated flexible wearable TEGs, as well as validate them for thermoelectric energy harvesting from the human body.

1.4 Research Scopes

The purpose of this research is to design and fabricate flexible wearable TEGs integrated with vertically aligned PEDOT:PSS and SWCNT film thermoelements. In this study, COMSOL Multiphysics[®] was used to perform finite element analysis (FEA) on the PEDOT:PSS and SWCNT thin films in order to determine their optimal length in order to attain the maximum ΔT for thermoelectric energy harvesting from the human body. Throughout the simulation, the electrical properties of the PEDOT:PSS and SWCNT films were assumed to be constant with increasing temperature. Moreover, no convection or heat radiation losses to the environment were accounted for on all surfaces of the PEDOT:PSS and SWCNT films. In terms of the synthesis of the PEDOT:PSS and SWCNT thin films, this study followed standard techniques, including solution-processing and drop-cast techniques. Meanwhile, SolidWorks[®], 3D printing and sacrificial molding techniques were utilized to design and develop the TEG structures with the desired dimensions based on polydimethylsiloxane (PDMS).

To characterize the morphological properties of the PEDOT:PSS film, a scanning electron microscope (SEM) was utilized. On the other hand, a field-emission scanning electron microscope (FESEM) was used to characterize the morphological properties of the SWCNT film, inspect their homogeneity, and determine the diameter of specific nanotube branches or bundle networks. A laboratory-built measurement setup was used for characterization of the synthesized PEDOT:PSS and SWCNT thin films, as well as the fabricated TEGs, and to validate the performance of TEGs for thermoelectric energy harvesting from the human body. The measurement setup

includes an infrared thermal camera, a hot plate, an aluminum heatsink, a computer, and a digital multimeter. The infrared images of the temperature distribution profile over the TEGs were captured to determine their ΔT to ease the characterization process.

1.5 Research Significances

Wearable electronics, which include electronic skins, smart band-aids, and health monitoring sensors, have emerged as a prevalent category of devices in today's technological landscape. These devices are widely utilized to monitor human physiological conditions non-invasively, allowing for early detection of health complications and the provision of tailored medical treatment. Regrettably, the absence of a stable, compact power supply is a major concern for most of the devices. While renewable energy sources have the potential to be used as a way to solve the issue, nonetheless, on-board sustainable energy harvester-based electronic devices are exceedingly rare due to their complex operating mechanisms, size, and high cost. To address this issue of constant power, TEG has been considered as a promising sustainable option that has the potential to replace a battery entirely or work in conjunction with conventional batteries to power a variety of wearable devices. This research predominantly discusses the detailed TEG working mechanism to generate useable power and its optimization factors, which include both device configurations and novel breakthrough thermoelectric materials that are pertinent to various applications. In addition, this research delves into the details of promising inorganic and organic materials with thermoelectric properties, including S , σ , t , and ZT . More precisely, this research investigated ways to increase power generation via architectural solutions and thermoelement length optimizations. The proposed flexible wearable TEG with vertically aligned PEDOT:PSS and SWCNT thin film thermoelements overcomes the limitation of continuous power generation. Since the thermoelements were constructed using inexpensive fabrication techniques, the overall cost of the TEGs was also reduced. Eventually, the low-cost TEGs could contribute significantly to the development of sustainable energy harvesting for wearable electronics via body heat, resulting in self-powered devices.

1.6 Thesis Outlines

This thesis is comprised of six chapters, each of which makes a significant contribution to the overall thesis. Chapter 1 outlines the background of the study, including the need for self-powered wearable and biomedical devices, as well as the potential for energy harvesters, particularly TEG, to power such devices. In addition, the problem statements are presented, followed by the objectives, scopes, and potential impacts of the research.

Chapter 2 begins with an overview of the energy harvesters, followed by the fundamental working mechanism of the TEG and its associated equations. This chapter included a comprehensive and in-depth review of the literature regarding the classification of TEGs based on the heat flow and layout of thermoelement pairs. Moreover, the previous work on both high-performance inorganic and organic thermoelectric materials is also reviewed. The chapter concludes with a discussion of the challenges associated with the concurrent TEG and research plans for this study.

Chapter 3 delves into the research methodology used to accomplish the objectives of the study. It details the design of the TEGs and FEA studies for the PEDOT:PSS and SWCNT thin films. Moreover, the experimental setup and characterization details for the study are included at the end of the chapter.

Chapter 4 presents a novel vertically aligned PEDOT:PSS thin film thermoelement integrated wearable TEG. Starting with the FEA to optimize and determine of the heat distribution through the PEDOT:PSS thermoelement, the design of the novel TEG structure is presented. The synthesis of the PEDOT:PSS material and TEG fabrication processes is also discussed. An experimental setup is built to characterize the thermoelectric properties, mainly α and S values, of the PEDOT:PSS film and to evaluate the TEG characterization results. Eventually, energy harvesting from the wrist via the fabricated TEG is demonstrated.

Likewise, in Chapter 5, vertically aligned PEDOT:PSS and SWCNT thin film thermoelements are integrated into a novel wearable TEG. It also covers the FEA for

optimizing and determining heat transfer through PEDOT:PSS and SWCNT thin film thermoelements, TEG structural design, as well as synthesis of the thermoelectric materials and TEG fabrication processes. The experimental setup is described, as are the results of materials characterization and device fabrication. Finally, energy harvesting from the wrist using the TEG is demonstrated.

The key findings of this research and the research contributions to this study are summarized in Chapter 6. Recommendations for future work are made to assist others in developing this technology and enhance the quality of this work.

REFERENCES

- [1] H. C. Koydemir and A. Ozcan, "Wearable and implantable sensors for biomedical applications," *Annual Review of Analytical Chemistry*, vol. 11, pp. 127-146, 2018.
- [2] Gu, Y., Zhang, T., Chen, H., Wang, F., Pu, Y., Gao, C. and Li, S., "Mini review on flexible and wearable electronics for monitoring human health information," *Nanoscale Research Letters*, vol. 14, no. 1, pp. 1-15, 2019.
- [3] Li, Y., Chen, W. and Lu, L., "Wearable and Biodegradable Sensors for Human Health Monitoring," *ACS Applied Bio Materials*, vol. 4, no. 1, pp. 122-139, 2020.
- [4] Haghi, M., Neubert, S., Geissler, A., Fleischer, H., Stoll, N., Stoll, R. and Thurow, K., "A flexible and pervasive IoT-based healthcare platform for physiological and environmental parameters monitoring," *IEEE Internet of Things Journal*, vol. 7, no. 6, pp. 5628-5647, 2020.
- [5] Haghi, M., Danyali, S., Ayasseh, S., Wang, J., Aazami, R. and Deserno, T. M., "Wearable devices in health monitoring from the environmental towards multiple domains: A survey," *Sensors*, vol. 21, no. 6, p. 2130, 2021.
- [6] C. Antzelevitch and A. Burashnikov, "Overview of basic mechanisms of cardiac arrhythmia," *Cardiac Electrophysiology Clinics*, vol. 3, no. 1, pp. 23-45, 2011.
- [7] G. Tse, "Mechanisms of cardiac arrhythmias," *Journal of Arrhythmia*, vol. 32, no. 2, pp. 75-81, 2016.
- [8] Dieffenderfer, J., Goodell, H., Mills, S., McKnight, M., Yao, S., Lin, F., Beppler, E., Bent, B., Lee, B., Misra, V. and Zhu, Y., "Low-power wearable systems for continuous monitoring of environment and health for chronic respiratory disease," *IEEE Journal of Biomedical and Health Informatics*, vol. 20, no. 5, pp. 1251-1264, 2016.
- [9] García Núñez, C., Manjakkal, L., Dahiya, R., "Energy autonomous electronic skin," *npj Flexible Electronics*, vol. 3, no. 1, pp. 1-24, 2019.
- [10] Zhan, Z., Lin, R., Tran, V.T., An, J., Wei, Y., Du, H., Tran, T. and Lu, W., "Paper/carbon nanotube-based wearable pressure sensor for physiological

- signal acquisition and soft robotic skin," *ACS Applied Materials & Interfaces*, vol. 9, no. 43, pp. 37921-37928, 2017.
- [11] Vaz, A., Ubarretxena, A., Zalbide, I., Pardo, D., Solar, H., Garcia-Alonso, A. and Berenguer, R., "Full passive UHF tag with a temperature sensor suitable for human body temperature monitoring," *IEEE Transactions on Circuits and Systems II: Express Briefs*, vol. 57, no. 2, pp. 95-99, 2010.
- [12] Liao, Y.T., Yao, H., Lingley, A., Parviz, B. and Otis, B.P., "A 3- μ W CMOS Glucose Sensor for Wireless Contact-Lens Tear Glucose Monitoring," *IEEE Journal of Solid-State Circuits*, vol. 47, no. 1, pp. 335-344, 2011.
- [13] Fan, X., Liu, B., Ding, J., Deng, Y., Han, X., Hu, W. and Zhong, C., "Flexible and Wearable Power Sources for Next-Generation Wearable Electronics," *Batteries & Supercaps*, vol. 3, no. 12, pp. 1262-1274, 2020.
- [14] Zhao, C, Lu, Y, Chen, L, Hu, and Y-S., "Flexible Na batteries," *InfoMat*, vol. 2, no. 1, pp. 126-138, 2020.
- [15] Guo, Z., Ma, Y., Dong, X., Huang, J., Wang, Y. and Xia, Y., "An environmentally friendly and flexible aqueous zinc battery using an organic cathode," *Angewandte Chemie*, vol. 130, no. 36, pp. 11911-11915, 2018.
- [16] Chen, J., Oh, S.K., Nabulsi, N., Johnson, H., Wang, W. and Ryou, J.H., "Biocompatible and sustainable power supply for self-powered wearable and implantable electronics using III-nitride thin-film-based flexible piezoelectric generator," *Nano Energy*, vol. 57, pp. 670-679, 2019.
- [17] Zheng, Q., Shi, B., Li, Z. and Wang, Z.L., "Recent progress on piezoelectric and triboelectric energy harvesters in biomedical systems," *Advanced Science*, vol. 4, no. 7, p. 1700029, 2017.
- [18] Dagdeviren, C., Li, Z. and Wang, Z.L., "Energy harvesting from the animal/human body for self-powered electronics," *Annual Review of Biomedical Engineering*, vol. 19, pp. 85-108, 2017.
- [19] Zhang, Q., Zhang, Z., Liang, Q., Gao, F., Yi, F., Ma, M., Liao, Q., Kang, Z. and Zhang, Y., "Green hybrid power system based on triboelectric nanogenerator for wearable/portable electronics," *Nano Energy*, vol. 55, pp. 151-163, 2019.
- [20] Li, Z., Zheng, Q., Wang, Z.L. and Li, Z., "Nanogenerator-based self-powered sensors for wearable and implantable electronics," *Research*, 8710686, 2020.

- [21] Ouyang, Q., Feng, X., Kuang, S., Panwar, N., Song, P., Yang, C., Yang, G., Hemu, X., Zhang, G., Yoon, H.S. and Tam, J.P., "Self-powered, on-demand transdermal drug delivery system driven by triboelectric nanogenerator," *Nano Energy*, vol. 62, pp. 610-619, 2019.
- [22] Liu, S., Hu, B., Liu, D., Li, F., Li, J.F., Li, B., Li, L., Lin, Y.H. and Nan, C.W., "Micro-thermoelectric generators based on through glass pillars with high output voltage enabled by large temperature difference," *Applied Energy*, vol. 225, pp. 600-610, 2018.
- [23] He, W., Zhang, G., Zhang, X., Ji, J., Li, G. and Zhao, X., "Recent development and application of thermoelectric generator and cooler," *Applied Energy*, vol. 143, pp. 1-25, 2015.
- [24] Kim, C.S., Lee, G.S., Choi, H., Kim, Y.J., Yang, H.M., Lim, S.H., Lee, S.G. and Cho, B.J., "Structural design of a flexible thermoelectric power generator for wearable applications," *Applied Energy*, vol. 214, pp. 131-138, 2018.
- [25] Ouyang, H., Liu, Z., Li, N., Shi, B., Zou, Y., Xie, F., Ma, Y., Li, Z., Li, H., Zheng, Q. and Qu, X., "Symbiotic cardiac pacemaker," *Nature Communications*, vol. 10, no. 1, pp. 1-10, 2019.
- [26] Yang, L., Ma, Z., Tian, Y., Meng, B. and Peng, Z., "Progress on Self-Powered Wearable and Implantable Systems Driven by Nanogenerators," *Micromachines*, vol. 12, no. 6, p. 666, 2021.
- [27] Kim, D.H., Shin, H.J., Lee, H., Jeong, C.K., Park, H., Hwang, G.T., Lee, H.Y., Joe, D.J., Han, J.H., Lee, S.H. and Kim, J., "In vivo self-powered wireless transmission using biocompatible flexible energy harvesters," *Advanced Functional Materials*, vol. 27, no. 25, p. 1700341, 2017.
- [28] Cheng, X., Xue, X., Ma, Y., Han, M., Zhang, W., Xu, Z., Zhang, H. and Zhang, H., "Implantable and self-powered blood pressure monitoring based on a piezoelectric thinfilm: Simulated, in vitro and in vivo studies," *Nano Energy*, vol. 22, pp. 453-460, 2016.
- [29] Zhu, L., Wang, Y., Mei, D. and Wu, X., "Highly sensitive and flexible tactile sensor based on porous graphene sponges for distributed tactile sensing in monitoring human motions," *Journal of Microelectromechanical Systems*, vol. 28, no. 1, pp. 154-163, 2018.
- [30] Liu, Z., Ma, Y., Ouyang, H., Shi, B., Li, N., Jiang, D., Xie, F., Qu, D., Zou, Y., Huang, Y. and Li, H., "Transcatheter self-powered ultrasensitive endocardial

- pressure sensor," *Advanced Functional Materials*, vol. 29, no. 3, p. 1807560, 2019.
- [31] Liu, Z., Nie, J., Miao, B., Li, J., Cui, Y., Wang, S., Zhang, X., Zhao, G., Deng, Y., Wu, Y. and Li, Z., "Self-powered intracellular drug delivery by a biomechanical energy-driven triboelectric nanogenerator," *Advanced Materials*, vol. 31, no. 12, p. 1807795, 2019.
- [32] Huang, T., Zhang, J., Yu, B., Yu, H., Long, H., Wang, H., Zhang, Q. and Zhu, M., "Fabric texture design for boosting the performance of a knitted washable textile triboelectric nanogenerator as wearable power," *Nano Energy*, vol. 58, pp. 375-383, 2019.
- [33] Zeng, H., He, H., Fu, Y., Zhao, T., Han, W., Xing, L., Zhang, Y., Zhan, Y. and Xue, X., "A self-powered brain-linked biosensing electronic-skin for actively tasting beverage and its potential application in artificial gustation," *Nanoscale*, vol. 10, no. 42, pp. 19987-19994, 2018.
- [34] Zhang, D., Wang, Y. and Yang, Y., "Design, performance, and application of thermoelectric nanogenerators," *Small*, vol. 15, no. 32, p. 1805241, 2019.
- [35] Malakooti, M.H., Kazem, N., Yan, J., Pan, C., Markvicka, E.J., Matyjaszewski, K. and Majidi, C., "Liquid metal supercooling for low-temperature thermoelectric wearables," *Advanced Functional Materials*, vol. 29, no. 45, p. 1906098, 2019.
- [36] Hu, G., Edwards, H. and Lee, M., "Silicon integrated circuit thermoelectric generators with a high specific power generation capacity," *Nature Electronics*, vol. 2, no. 7, pp. 300-306, 2019.
- [37] Yan, J., Liao, X., Yan, D. and Chen, Y., "Review of micro thermoelectric generator," *Journal of Microelectromechanical Systems*, vol. 27, no. 1, pp. 1-18, 2018.
- [38] Zhao, X., Zhao, C., Jiang, Y., Ji, X., Kong, F., Lin, T., Shao, H. and Han, W., "Flexible cellulose nanofiber/Bi₂Te₃ composite film for wearable thermoelectric devices," *Journal of Power Sources*, vol. 479, p. 229044, 2020.
- [39] Kong, D., Zhu, W., Guo, Z. and Deng, Y., "High-performance flexible Bi₂Te₃ films based wearable thermoelectric generator for energy harvesting," *Energy*, vol. 175, pp. 292-299, 2019.
- [40] Newbrook, D.W., Richards, S.P., Greenacre, V.K., Hector, A.L., Levason, W., Reid, G., de Groot, C.K. and Huang, R., "Selective Chemical Vapor Deposition

- Approach for Sb₂Te₃ Thin Film Micro-thermoelectric Generators," *ACS Applied Energy Materials*, vol. 3, no. 6, pp. 5840-5846, 2020.
- [41] Nozariasbmarz, A., Suarez, F., Dycus, J.H., Cabral, M.J., LeBeau, J.M., Öztürk, M.C. and Vashaee, D., "Thermoelectric generators for wearable body heat harvesting: Material and device concurrent optimization," *Nano Energy*, vol. 67, p. 104265, 2020.
- [42] Hasan, M.N., Nafea, M., Nayan, N. and Mohamed Ali, M.S., "Thermoelectric Generator: Materials and Applications in Wearable Health Monitoring Sensors and Internet of Things Devices," *Advanced Materials Technologies*, p. 2101203, 2021.
- [43] Liu, D., Yan, Z., Zhao, Y., Zhang, Z., Zhen, Y., Zhang, B., Shi, P. and Xue, C., "Facile MWCNTs-SnSe/PEDOT: PSS ternary composite flexible thermoelectric films optimized by cold-pressing," *Journal of Materials Research and Technology*, 15, 4452-4460, 2021.
- [44] Kim, C.S., Yang, H.M., Lee, J., Lee, G.S., Choi, H., Kim, Y.J., Lim, S.H., Cho, S.H. and Cho, B.J., "Self-powered wearable electrocardiography using a wearable thermoelectric power generator," *ACS Energy Letters*, vol. 3, no. 3, pp. 501-507, 2018.
- [45] Wang, T., Ji, T., Chen, W., Li, X., Guan, W., Geng, Y., Wang, X., Li, Y. and Kang, Z., "Polyoxometalate film simultaneously converts multiple low-value all-weather environmental energy to electricity," *Nano Energy*, vol. 68, p. 104349, 2020.
- [46] Cheng, H., Du, Y., Wang, B., Mao, Z., Xu, H., Zhang, L., Zhong, Y., Jiang, W., Wang, L. and Sui, X., "Flexible cellulose-based thermoelectric sponge towards wearable pressure sensor and energy harvesting," *Chemical Engineering Journal*, vol. 338, pp. 1-7, 2018.
- [47] Li, X., Feng, Q., Lu, K., Huang, J., Zhang, Y., Hou, Y., Qiao, H., Li, D. and Wei, Q., "Encapsulating enzyme into metal-organic framework during in-situ growth on cellulose acetate nanofibers as self-powered glucose biosensor," *Biosensors and Bioelectronics*, vol. 171, p. 112690, 2021.
- [48] Li, X., Tat, T. and Chen, J., "Triboelectric nanogenerators for self-powered drug delivery," *Trends in Chemistry*, 3(9), 765, 2021.
- [49] Bandyopadhyay, S., Mercier, P.P., Lysaght, A.C., Stankovic, K.M. and Chandrakasan, A.P., "A 1.1 nW energy-harvesting system with 544 pW

- quiescent power for next-generation implants," *IEEE journal of Solid-State Circuits*, vol. 49, no. 12, pp. 2812-2824, 2014.
- [50] H. Dinis and P. Mendes, "A comprehensive review of powering methods used in state-of-the-art miniaturized implantable electronic devices," *Biosensors and Bioelectronics*, vol. 172, p. 112781, 2021.
- [51] Yang, S.Y., Sencadas, V., You, S.S., Jia, N.Z.X., Srinivasan, S.S., Huang, H.W., Ahmed, A.E., Liang, J.Y. and Traverso, G., "Powering Implantable and Ingestible Electronics," *Advanced Functional Materials*, p. 2009289, 2021.
- [52] Cho, S., Yun, Y., Jang, S., Ra, Y., Choi, J.H., Hwang, H.J., Choi, D. and Choi, D., "Universal biomechanical energy harvesting from joint movements using a direction-switchable triboelectric nanogenerator," *Nano Energy*, vol. 71, p. 104584, 2020.
- [53] Shi, Y., Lü, X., Xiang, Q., Li, J., Shao, X. and Bao, W., "Stretchable thermoelectric generator for wearable power source and temperature detection applications," *Energy Conversion and Management*, vol. 253, p. 115167, 2022.
- [54] Sun, C., Shi, J., Bayerl, D.J. and Wang, X., "PVDF microbelts for harvesting energy from respiration," *Energy & Environmental Science*, vol. 4, no. 11, pp. 4508-4512, 2011.
- [55] D. Champier, "Thermoelectric generators: A review of applications," *Energy Conversion and Management*, vol. 140, pp. 167-181, 2017.
- [56] Zoui, M.A., Bentouba, S., Stocholm, J.G. and Bourouis, M., "A review on thermoelectric generators: Progress and applications," *Energies*, vol. 13, no. 14, p. 3606, 2020.
- [57] Selvan, K.V., Hasan, M.N. and Mohamed Ali, M.S., "State-of-the-art reviews and analyses of emerging research findings and achievements of thermoelectric materials over the past years," *Journal of Electronic Materials*, vol. 48, no. 2, pp. 745-777, 2019.
- [58] Selvan, K.V., Hasan, M.N. and Mohamed Ali, M.S., "Methodological reviews and analyses on the emerging research trends and progresses of thermoelectric generators," *International Journal of Energy Research*, vol. 43, no. 1, pp. 113-140, 2019.
- [59] Jaziri, N., Boughamoura, A., Müller, J., Mezghani, B., Tounsi, F. and Ismail, M., "A comprehensive review of Thermoelectric Generators: Technologies and common applications," *Energy Reports*, vol. 6, pp. 264-287, 2020.

- [60] Kim, S.J., Choi, H., Kim, Y., We, J.H., Shin, J.S., Lee, H.E., Oh, M.W., Lee, K.J. and Cho, B.J., "Post ionized defect engineering of the screen-printed $\text{Bi}_2\text{Te}_{2.7}\text{Se}_{0.3}$ thick film for high performance flexible thermoelectric generator," *Nano Energy*, vol. 31, pp. 258-263, 2017.
- [61] Jaldurgam, F.F., Ahmad, Z. and Touati, F., "Synthesis and Performance of Large-Scale Cost-Effective Environment-Friendly Nanostructured Thermoelectric Materials," *Nanomaterials*, vol. 11, no. 5, p. 1091, 2021.
- [62] Kim, J., Khan, S., Wu, P., Park, S., Park, H., Yu, C. and Kim, W., "Self-charging wearables for continuous health monitoring," *Nano Energy*, vol. 79, p. 105419, 2021.
- [63] Yuan, J., Zhu, R. and Li, G., "Self-Powered Electronic Skin with Multisensory Functions Based on Thermoelectric Conversion," *Advanced Materials Technologies*, vol. 5, no. 9, p. 2000419, 2020.
- [64] J. Yuan and R. Zhu, "A fully self-powered wearable monitoring system with systematically optimized flexible thermoelectric generator," *Applied Energy*, vol. 271, p. 115250, 2020.
- [65] Chen, M.D., Wang, J.Y., Yang, S.M. and Tsai, M.H., "Structural design for dimensional stability of thermocouples in thermoelectric energy harvester," *IEEE Sensors Journal*, vol. 19, no. 1, pp. 58-64, 2018.
- [66] Zhan, T., Yamato, R., Hashimoto, S., Tomita, M., Oba, S., Himeda, Y., Mesaki, K., Takezawa, H., Yokogawa, R., Xu, Y. and Matsukawa, T., "Miniaturized planar Si-nanowire micro-thermoelectric generator using exuded thermal field for power generation," *Science and Technology of advanced MaTerialS*, vol. 19, no. 1, pp. 443-453, 2018.
- [67] Aktakka, E.E., Ghafouri, N., Smith, C.E., Peterson, R.L., Hussain, M.M. and Najafi, K., "Post-CMOS FinFET integration of bismuth telluride and antimony telluride thin-film-based thermoelectric devices on SoI substrate," *IEEE Electron Device Letters*, vol. 34, no. 10, pp. 1334-1336, 2013.
- [68] L. K. Allison and T. L. Andrew, "A wearable all-fabric thermoelectric generator," *Advanced Materials Technologies*, vol. 4, no. 5, p. 1800615, 2019.
- [69] H. Song and K. Cai, "Preparation and properties of PEDOT:PSS/Te nanorod composite films for flexible thermoelectric power generator," *Energy*, vol. 125, pp. 519-525, 2017.

- [70] Zhang, Z., Qiu, J. and Wang, S., "Roll-to-roll printing of flexible thin-film organic thermoelectric devices," *Manufacturing Letters*, vol. 8, pp. 6-10, 2016.
- [71] Liu, D., Yan, Z., Zhao, Y., Zhang, Z., Zhen, Y., Zhang, B., Shi, P. and Xue, C., "Facile MWCNTs-SnSe/PEDOT:PSS ternary composite flexible thermoelectric films optimized by cold-pressing," *Journal of Materials Research and Technology*, vol. 15, pp. 4452-4460, 2021.
- [72] Wen, N., Fan, Z., Yang, S., Zhao, Y., Li, C., Cong, T., Huang, H., Zhang, J., Guan, X. and Pan, L., "High-performance stretchable thermoelectric fibers for wearable electronics," *Chemical Engineering Journal*, p. 130816, 2021.
- [73] Wen, N., Fan, Z., Yang, S., Zhao, Y., Cong, T., Xu, S., Zhang, H., Wang, J., Huang, H., Li, C. and Pan, L., "Highly conductive, ultra-flexible and continuously processable PEDOT:PSS fibers with high thermoelectric properties for wearable energy harvesting," *Nano Energy*, vol. 78, p. 105361, 2020.
- [74] Wang, C., Sun, K., Fu, J., Chen, R., Li, M., Zang, Z., Liu, X., Li, B., Gong, H. and Ouyang, J., "Enhancement of conductivity and thermoelectric property of PEDOT:PSS via acid doping and single post-treatment for flexible power generator," *Advanced Sustainable Systems*, vol. 2, no. 12, p. 1800085, 2018.
- [75] Tomita, M., Oba, S., Himeda, Y., Yamato, R., Shima, K., Kumada, T., Xu, M., Takezawa, H., Mesaki, K., Tsuda, K. and Hashimoto, S., "Modeling, Simulation, Fabrication, and Characterization of a 10- μ W/cm² Class Si-Nanowire Thermoelectric Generator for IoT Applications," *IEEE Transactions on Electron Devices*, vol. 65, no. 11, pp. 5180-5188, 2018.
- [76] Biswas, K., He, J., Zhang, Q., Wang, G., Uher, C., Dravid, V.P. and Kanatzidis, M.G., "Strained endotaxial nanostructures with high thermoelectric figure of merit," *Nature chemistry*, vol. 3, no. 2, pp. 160-166, 2011.
- [77] Witting, I.T., Chasapis, T.C., Ricci, F., Peters, M., Heinz, N.A., Hautier, G. and Snyder, G.J., "The thermoelectric properties of bismuth telluride," *Advanced Electronic Materials*, vol. 5, no. 6, p. 1800904, 2019.
- [78] Wang, W., Sun, Y., Feng, Y., Qin, H., Zhu, J., Guo, F., Cai, W. and Sui, J., "High thermoelectric performance bismuth telluride prepared by cold pressing and annealing facilitating large scale application," *Materials Today Physics*, vol. 21, p. 100522, 2021.

- [79] Hosokawa, Y., Tomita, K. and Takashiri, M., "Growth of single-crystalline Bi₂Te₃ hexagonal nanoplates with and without single nanopores during temperature-controlled solvothermal synthesis," *Scientific Reports*, vol. 9, no. 1, pp. 1-7, 2019.
- [80] Tang, X., Xie, W., Li, H., Zhao, W., Zhang, Q. and Niino, M., "Preparation and thermoelectric transport properties of high-performance *p*-type Bi₂Te₃ with layered nanostructure," *Applied Physics Letters*, vol. 90, no. 1, p. 012102, 2007.
- [81] Hu, L., Zhu, T., Liu, X. and Zhao, X., "Point defect engineering of high-performance bismuth-telluride-based thermoelectric materials," *Advanced Functional Materials*, vol. 24, no. 33, pp. 5211-5218, 2014.
- [82] Kim, K.T., Min, T.S., Kim, S.D., Choi, E.A., Kim, D.W. and Choi, S.Y., "Strain-mediated point defects in thermoelectric *p*-type bismuth telluride polycrystalline," *Nano Energy*, vol. 55, pp. 486-493, 2019.
- [83] Kim, S.I., Lee, K.H., Mun, H.A., Kim, H.S., Hwang, S.W., Roh, J.W., Yang, D.J., Shin, W.H., Li, X.S., Lee, Y.H. and Snyder, G.J., "Dense dislocation arrays embedded in grain boundaries for high-performance bulk thermoelectrics," *Science*, vol. 348, no. 6230, pp. 109-114, 2015.
- [84] Yu, Y., He, D.S., Zhang, S., Cojocaru-Mirédin, O., Schwarz, T., Stoffers, A., Wang, X.Y., Zheng, S., Zhu, B., Scheu, C. and Wu, D., "Simultaneous optimization of electrical and thermal transport properties of Bi_{0.5}Sb_{1.5}Te₃ thermoelectric alloy by twin boundary engineering," *Nano Energy*, vol. 37, pp. 203-213, 2017.
- [85] Madavali, B., Kim, H.S., Lee, K.H. and Hong, S.J., "Enhanced Seebeck coefficient by energy filtering in Bi-Sb-Te based composites with dispersed Y₂O₃ nanoparticles," *Intermetallics*, vol. 82, pp. 68-75, 2017.
- [86] Cai, B., Hu, H., Zhuang, H.L. and Li, J.F., "Promising materials for thermoelectric applications," *Journal of Alloys and Compounds*, vol. 806, pp. 471-486, 2019.
- [87] Zhao, L.D., Lo, S.H., Zhang, Y., Sun, H., Tan, G., Uher, C., Wolverton, C., Dravid, V.P. and Kanatzidis, M.G., "Ultralow thermal conductivity and high thermoelectric figure of merit in SnSe crystals," *Nature*, vol. 508, no. 7496, pp. 373-377, 2014.

- [88] Chen, Z.G., Shi, X., Zhao, L.D. and Zou, J., "High-performance SnSe thermoelectric materials: Progress and future challenge," *Progress in Materials Science*, vol. 97, pp. 283-346, 2018.
- [89] Shi, W., Gao, M., Wei, J., Gao, J., Fan, C., Ashalley, E., Li, H. and Wang, Z., "Tin selenide (SnSe): growth, properties, and applications," *Advanced Science*, vol. 5, no. 4, p. 1700602, 2018.
- [90] Duong, A.T., Nguyen, V.Q., Duvjir, G., Duong, V.T., Kwon, S., Song, J.Y., Lee, J.K., Lee, J.E., Park, S., Min, T. and Lee, J., "Achieving $ZT=2.2$ with Bi-doped *n*-type SnSe single crystals," *Nature Communications*, vol. 7, no. 1, pp. 1-6, 2016.
- [91] Chang, C., Wu, M., He, D., Pei, Y., Wu, C.F., Wu, X., Yu, H., Zhu, F., Wang, K., Chen, Y. and Huang, L., "3D charge and 2D phonon transports leading to high out-of-plane ZT in *n*-type SnSe crystals," *Science*, vol. 360, no. 6390, pp. 778-783, 2018.
- [92] Chu, F., Zhang, Q., Zhou, Z., Hou, D., Wang, L. and Jiang, W., "Enhanced thermoelectric and mechanical properties of Na-doped polycrystalline SnSe thermoelectric materials via CNTs dispersion," *Journal of Alloys and Compounds*, vol. 741, pp. 756-764, 2018.
- [93] Shi, X., Wu, A., Feng, T., Zheng, K., Liu, W., Sun, Q., Hong, M., Pantelides, S.T., Chen, Z.G. and Zou, J., "High thermoelectric performance in *p*-type polycrystalline cd-doped SnSe achieved by a combination of cation vacancies and localized lattice engineering," *Advanced Energy Materials*, vol. 9, no. 11, p. 1803242, 2019.
- [94] Li, C., Wu, H., Zhang, B., Zhu, H., Fan, Y., Lu, X., Sun, X., Zhang, X., Wang, G. and Zhou, X., "High Thermoelectric Performance of Co-Doped *p*-Type Polycrystalline SnSe via Optimizing Electrical Transport Properties," *ACS Applied Materials & Interfaces*, vol. 12, no. 7, pp. 8446-8455, 2020.
- [95] Zhao, Q., Qin, B., Wang, D., Qiu, Y. and Zhao, L.D., "Realizing high thermoelectric performance in polycrystalline SnSe via silver doping and germanium alloying," *ACS Applied Energy Materials*, vol. 3, no. 3, pp. 2049-2054, 2019.
- [96] Yu, B., Liu, W., Chen, S., Wang, H., Wang, H., Chen, G. and Ren, Z., "Thermoelectric properties of copper selenide with ordered selenium layer and disordered copper layer," *Nano Energy*, vol. 1, no. 3, pp. 472-478, 2012.

- [97] Kim, H., Ballikaya, S., Chi, H., Ahn, J.P., Ahn, K., Uher, C. and Kaviani, M., "Ultralow thermal conductivity of Cu_2Se by atomic fluidity and structure distortion," *Acta Materialia*, vol. 86, pp. 247-253, 2015.
- [98] Yang, L., Chen, Z.G., Han, G., Hong, M., Zou, Y. and Zou, J., "High-performance thermoelectric Cu_2Se nanoplates through nanostructure engineering," *Nano Energy*, vol. 16, pp. 367-374, 2015.
- [99] Gahtori, B., Bathula, S., Tyagi, K., Jayasimhadri, M., Srivastava, A.K., Singh, S., Budhani, R.C. and Dhar, A., "Giant enhancement in thermoelectric performance of copper selenide by incorporation of different nanoscale dimensional defect features," *Nano Energy*, vol. 13, pp. 36-46, 2015.
- [100] Zhao, K., Qiu, P., Song, Q., Blichfeld, A.B., Eikeland, E., Ren, D., Ge, B., Iversen, B.B., Shi, X. and Chen, L., "Ultrahigh thermoelectric performance in $\text{Cu}_{2-y}\text{Se}_{0.5}\text{S}_{0.5}$ liquid-like materials," *Materials Today Physics*, vol. 1, pp. 14-23, 2017.
- [101] Li, M., Islam, S.M.K.N., Yahyaoglu, M., Pan, D., Shi, X., Chen, L., Aydemir, U. and Wang, X., "Ultrahigh figure-of-merit of Cu_2Se incorporated with carbon coated boron nanoparticles," *InfoMat*, vol. 1, no. 1, pp. 108-115, 2019.
- [102] Zhao, L., Islam, S.M.K.N., Wang, J., Cortie, D.L., Wang, X., Cheng, Z., Wang, J., Ye, N., Dou, S., Shi, X. and Chen, L., "Significant enhancement of figure-of-merit in carbon-reinforced Cu_2Se nanocrystalline solids," *Nano Energy*, vol. 41, pp. 164-171, 2017.
- [103] Li, M., Cortie, D.L., Liu, J., Yu, D., Islam, S.M.K.N., Zhao, L., Mitchell, D.R., Mole, R.A., Cortie, M.B., Dou, S. and Wang, X., "Ultra-high thermoelectric performance in graphene incorporated Cu_2Se : Role of mismatching phonon modes," *Nano Energy*, vol. 53, pp. 993-1002, 2018.
- [104] Yu, K., Zhou, Y., Liu, Y., Liu, F., Hu, L., Ao, W., Zhang, C., Li, Y., Li, J. and Xie, H., "Near-room-temperature thermoelectric materials and their application prospects in geothermal power generation," *Geomechanics and Geophysics for Geo-Energy and Geo-Resources*, vol. 6, no. 1, p. 12, 2020.
- [105] Hasan, M.N., Rahim, H.A., Ahmad, M.A. and Ali, M.S.M., "Modelling and simulation of magnesium antimonide based thermoelectric generator," *Indonesian Journal of Electrical Engineering and Computer Science*, vol. 19, no. 2, pp. 686-692, 2020.

- [106] Cui, Y., Zhang, X., Duan, B., Li, J., Yang, H., Wang, H., Wen, P., Gao, T., Fang, Z., Li, G. and Li, Y., "Band structure and thermoelectric properties of Al-doped $\text{Mg}_{3-x}\text{Al}_x\text{Sb}_2$ compounds," *Journal of Materials Science: Materials in Electronics*, vol. 30, no. 16, pp. 15206-15213, 2019.
- [107] Meng, F., Sun, S., Ma, J., Chronister, C., He, J. and Li, W., "Anisotropic thermoelectric figure-of-merit in Mg_3Sb_2 ," *Materials Today Physics*, p. 100217, 2020.
- [108] A. Bhardwaj and D. Misra, "Enhancing thermoelectric properties of a p -type Mg_3Sb_2 -based Zintl phase compound by Pb substitution in the anionic framework," *Rsc Advances*, vol. 4, no. 65, pp. 34552-34560, 2014.
- [109] Song, L., Zhang, J. and Iversen, B.B., "Simultaneous improvement of power factor and thermal conductivity via Ag doping in p -type Mg_3Sb_2 thermoelectric materials," *Journal of Materials Chemistry a*, vol. 5, no. 10, pp. 4932-4939, 2017.
- [110] Tang, X., Zhang, B., Zhang, X., Wang, S., Lu, X., Han, G., Wang, G. and Zhou, X., "Enhancing the Thermoelectric Performance of p -Type Mg_3Sb_2 via Codoping of Li and Cd," *ACS Applied Materials & Interfaces*, vol. 12, no. 7, pp. 8359-8365, 2020.
- [111] Bhardwaj, A., Shukla, A.K., Dhakate, S.R. and Misra, D.K., "Graphene boosts thermoelectric performance of a Zintl phase compound," *RSC Advances*, vol. 5, no. 15, pp. 11058-11070, 2015.
- [112] Song, S.W., Mao, J., Bordelon, M., He, R., Wang, Y.M., Shuai, J., Sun, J.Y., Lei, X.B., Ren, Z.S., Chen, S. and Wilson, S., "Joint effect of magnesium and yttrium on enhancing thermoelectric properties of n -type Zintl $\text{Mg}_{3+\delta}\text{Y}_{0.02}\text{Sb}_{1.5}\text{Bi}_{0.5}$," *Materials Today Physics*, vol. 8, pp. 25-33, 2019.
- [113] Chen, X., Wu, H., Cui, J., Xiao, Y., Zhang, Y., He, J., Chen, Y., Cao, J., Cai, W., Pennycook, S.J. and Liu, Z., "Extraordinary thermoelectric performance in n -type manganese doped Mg_3Sb_2 Zintl: High band degeneracy, tuned carrier scattering mechanism and hierarchical microstructure," *Nano Energy*, vol. 52, pp. 246-255, 2018.
- [114] Wang, Y., Liu, W.D., Shi, X.L., Hong, M., Wang, L.J., Li, M., Wang, H., Zou, J. and Chen, Z.G., "Enhanced thermoelectric properties of nanostructured n -type Bi_2Te_3 by suppressing Te vacancy through non-equilibrium fast reaction," *Chemical Engineering Journal*, vol. 391, p. 123513, 2020.

- [115] Choi, H., Jeong, K., Chae, J., Park, H., Baeck, J., Kim, T.H., Song, J.Y., Park, J., Jeong, K.H. and Cho, M.H., "Enhancement in thermoelectric properties of Te-embedded Bi₂Te₃ by preferential phonon scattering in heterostructure interface," *Nano Energy*, vol. 47, pp. 374-384, 2018.
- [116] Li, J., Zhang, C., Feng, Y., Zhang, C., Li, Y., Hu, L., Ao, W. and Liu, F., "Effects on phase transition and thermoelectric properties in the Pb-doped GeTe-Bi₂Te₃ alloys with thermal annealing," *Journal of Alloys and Compounds*, vol. 808, p. 151747, 2019.
- [117] Russ, B., Glauddell, A., Urban, J.J., Chabinyk, M.L. and Segalman, R.A., "Organic thermoelectric materials for energy harvesting and temperature control," *Nature Reviews Materials*, vol. 1, no. 10, pp. 1-14, 2016.
- [118] Nandihalli, N., Liu, C.J. and Mori, T., "Polymer based thermoelectric nanocomposite materials and devices: Fabrication and characteristics," *Nano Energy*, p. 105186, 2020.
- [119] N. Dubey and M. Leclerc, "Conducting polymers: efficient thermoelectric materials," *Journal of Polymer Science Part B: Polymer Physics*, vol. 49, no. 7, pp. 467-475, 2011.
- [120] Zhang, Q., Sun, Y., Xu, W. and Zhu, D., "Organic thermoelectric materials: emerging green energy materials converting heat to electricity directly and efficiently," *Advanced Materials*, vol. 26, no. 40, pp. 6829-6851, 2014.
- [121] Bharti, M., Singh, A., Samanta, S. and Aswal, D.K., "Conductive polymers for thermoelectric power generation," *Progress in Materials Science*, vol. 93, pp. 270-310, 2018/04/01/ 2018.
- [122] Culebras, M., de Lima Jr, M.M., Gómez, C. and Cantarero, A., "Organic thermoelectric modules produced by electrochemical polymerization," *Journal of Applied Polymer Science*, vol. 134, no. 3, 2017.
- [123] Horta-Romarís, L., González-Rodríguez, M.V., Lasagabáster, A., Rivadulla, F. and Abad, M.J., "Thermoelectric properties and intrinsic conduction processes in DBSA and NaSIPA doped polyanilines," *Synthetic Metals*, vol. 243, pp. 44-50, 2018.
- [124] Park, Y.W., Moon, J.S., Bak, M.K. and Jin, J.I., "Electrical properties of polyaniline and substituted polyaniline derivatives," *Synthetic Metals*, vol. 29, no. 1, pp. 389-394, 1989.

- [125] Park, Y.W., Lee, Y.S., Park, C., Shacklette, L.W. and Baughman, R.H., "Thermopower and conductivity of metallic polyaniline," *Solid State Communications*, vol. 63, no. 11, pp. 1063-1066, 1987.
- [126] Li, J., Tang, X., Li, H., Yan, Y. and Zhang, Q., "Synthesis and thermoelectric properties of hydrochloric acid-doped polyaniline," *Synthetic Metals*, vol. 160, pp. 1153-1158, 2010.
- [127] Nath, C., Kumar, A., Kuo, Y.K. and Okram, G.S., "High thermoelectric figure of merit in nanocrystalline polyaniline at low temperatures," *Applied Physics Letters*, vol. 105, p. 133108, 2014.
- [128] Li, P., Zhao, Y., Li, H., Liu, S., Liang, Y., Cheng, X. and He, C., "Facile green strategy for improving thermoelectric performance of carbon nanotube/polyaniline composites by ethanol treatment," *Composites Science and Technology*, vol. 189, p. 108023, 2020.
- [129] Wang, H., Yin, L., Pu, X. and Yu, C., "Facile charge carrier adjustment for improving thermopower of doped polyaniline," *Polymer*, vol. 54, no. 3, pp. 1136-1140, 2013.
- [130] Sun, Y., Wei, Z., Xu, W. and Zhu, D., "A three-in-one improvement in thermoelectric properties of polyaniline brought by nanostructures," *Synthetic metals*, vol. 160, no. 21-22, pp. 2371-2376, 2010.
- [131] Chatterjee, K., Mitra, M., Ganguly, S., Kargupta, K. and Banerjee, D., "Thermoelectric performance of electrodeposited nanostructured polyaniline doped with sulfo-salicylic acid," *Journal of Applied Polymer Science*, vol. 131, no. 4, 2014.
- [132] Wu, J., Sun, Y., Xu, W. and Zhang, Q., "Investigating thermoelectric properties of doped polyaniline nanowires," *Synthetic Metals*, vol. 189, pp. 177-182, 2014.
- [133] Bubnova, O., Khan, Z.U., Malti, A., Braun, S., Fahlman, M., Berggren, M. and Crispin, X., "Optimization of the thermoelectric figure of merit in the conducting polymer poly (3, 4-ethylenedioxythiophene)," *Nature materials*, vol. 10, no. 6, p. 429, 2011.
- [134] Z. Fan and J. Ouyang, "Thermoelectric properties of PEDOT: PSS," *Advanced Electronic Materials*, vol. 5, no. 11, p. 1800769, 2019.

- [135] Wei, Q., Mukaida, M., Kirihara, K., Naitoh, Y. and Ishida, T., "Recent progress on PEDOT-based thermoelectric materials," *Materials*, vol. 8, no. 2, pp. 732-750, 2015.
- [136] Xu, Y., Liu, Z., Wei, X., Wu, J., Guo, J., Zhao, B., Wang, H., Chen, S. and Dou, Y., "Morphological modulation to improve thermoelectric performances of PEDOT: PSS films by DMSO vapor post-treatment," *Synthetic Metals*, vol. 271, p. 116628, 2021.
- [137] Xiong, J., Jiang, F., Zhou, W., Liu, C. and Xu, J., "Highly electrical and thermoelectric properties of a PEDOT: PSS thin-film via direct dilution-filtration," *RSC advances*, vol. 5, no. 75, pp. 60708-60712, 2015.
- [138] Yi, C., Wilhite, A., Zhang, L., Hu, R., Chuang, S.S., Zheng, J. and Gong, X., "Enhanced thermoelectric properties of poly (3, 4-ethylenedioxythiophene): poly (styrenesulfonate) by binary secondary dopants," *ACS Applied Materials & Interfaces*, vol. 7, no. 17, pp. 8984-8989, 2015.
- [139] Park, H., Lee, S.H., Kim, F.S., Choi, H.H., Cheong, I.W. and Kim, J.H., "Enhanced thermoelectric properties of PEDOT: PSS nanofilms by a chemical dedoping process," *Journal of Materials Chemistry A*, vol. 2, no. 18, pp. 6532-6539, 2014.
- [140] Lee, S.H., Park, H., Kim, S., Son, W., Cheong, I.W. and Kim, J.H., "Transparent and flexible organic semiconductor nanofilms with enhanced thermoelectric efficiency," *Journal of Materials Chemistry A*, vol. 2, no. 20, pp. 7288-7294, 2014.
- [141] Yemata, T.A., Zheng, Y., Kyaw, A.K.K., Wang, X., Song, J., Chin, W.S. and Xu, J., "Binary treatment of PEDOT: PSS films with nitric acid and imidazolium-based ionic liquids to improve the thermoelectric properties," *Materials Advances*, 2020.
- [142] Yemata, T.A., Kyaw, A.K.K., Zheng, Y., Wang, X., Zhu, Q., Chin, W.S. and Xu, J., "Enhanced thermoelectric performance of poly (3, 4-ethylenedioxythiophene): poly (4-styrenesulfonate)(PEDOT: PSS) with long-term humidity stability via sequential treatment with trifluoroacetic acid," *Polymer International*, vol. 69, no. 1, pp. 84-92, 2020.
- [143] Peng, S., Wang, D., Lu, J., He, M., Xu, C., Li, Y. and Zhu, S., "A Review on Organic Polymer-Based Thermoelectric Materials," *Journal of Polymers and the Environment*, vol. 25, no. 4, pp. 1208-1218, 2017.

- [144] Y. Lu and D. J. Young, "Coordination Polymers for *n*-Type Thermoelectric Applications," *Dalton Transactions*, 49(23):7644-57, 2020.
- [145] Sun, Y., Sheng, P., Di, C., Jiao, F., Xu, W., Qiu, D. and Zhu, D., "Organic Thermoelectric Materials and Devices Based on *p*-and *n*-Type Poly (metal 1, 1, 2, 2-ethenetetrathiolate) s," *Advanced Materials*, vol. 24, no. 7, pp. 932-937, 2012.
- [146] Jiao, F., Di, C.A., Sun, Y., Sheng, P., Xu, W. and Zhu, D., "Inkjet-printed flexible organic thin-film thermoelectric devices based on *p*-and *n*-type poly (metal 1, 1, 2, 2-ethenetetrathiolate) s/polymer composites through ball-milling," *Phil. Trans. R. Soc. A*, vol. 372, no. 2013, p. 20130008, 2014.
- [147] Cui, Y., Yan, J., Sun, Y., Zou, Y., Sun, Y., Xu, W. and Zhu, D., "Thermoelectric properties of metal-(Z)-1, 2-dihydroselenoethene-1, 2-dithiol coordination polymers," *Science Bulletin*, 2018.
- [148] Menon, A.K., Wolfe, R.M., Marder, S.R., Reynolds, J.R. and Yee, S.K., "Systematic Power Factor Enhancement in *n* Type NiETT/PVDF Composite Films," *Advanced Functional Materials*, p. 1801620, 2018.
- [149] Huang, X., Sheng, P., Tu, Z., Zhang, F., Wang, J., Geng, H., Zou, Y., Di, C.A., Yi, Y., Sun, Y. and Xu, W., "A two-dimensional π -d conjugated coordination polymer with extremely high electrical conductivity and ambipolar transport behaviour," *Nature Communications*, vol. 6, no. 1, pp. 1-8, 2015.
- [150] Cui, Y., Yan, J., Chen, Z., Zhang, J., Zou, Y., Sun, Y., Xu, W. and Zhu, D., "[Cu₃(C₆Se₆)]_n: The First Highly Conductive 2D π -d Conjugated Coordination Polymer Based on Benzenehexaselenolate," *Advanced Science*, vol. 6, no. 9, p. 1802235, 2019.
- [151] Huang, X., Qiu, Y., Wang, Y., Liu, L., Wu, X., Liang, Y., Cui, Y., Sun, Y., Zou, Y., Zhu, J. and Fang, W., "Highly Conducting Organic-inorganic Hybrid Copper Sulfides C_xC₆S₆ (X=4 or 5.5): Ligand-based Oxidation Induced Chemical and Electronic Structure Modulation," *Angewandte Chemie International Edition*, 132(50), pp.22791-22798, 2020.
- [152] Culebras, M., Choi, K. and Cho, C., "Recent progress in flexible organic thermoelectrics," *Micromachines*, vol. 9, no. 12, p. 638, 2018.
- [153] Wang, S., Liu, F., Gao, C., Wan, T., Wang, L., Wang, L. and Wang, L., "Enhancement of the thermoelectric property of nanostructured polyaniline/carbon nanotube composites by introducing pyrrole unit onto

- polyaniline backbone via a sustainable method," *Chemical Engineering Journal*, vol. 370, pp. 322-329, 2019.
- [154] Li, H., Liang, Y., Liu, S., Qiao, F., Li, P. and He, C., "Modulating carrier transport for the enhanced thermoelectric performance of carbon nanotubes/polyaniline composites," *Organic Electronics*, vol. 69, pp. 62-68, 2019.
- [155] Wang, L., Yao, Q., Xiao, J., Zeng, K., Qu, S., Shi, W., Wang, Q. and Chen, L., "Engineered molecular chain ordering in single-walled carbon nanotubes/polyaniline composite films for high-performance organic thermoelectric materials," *Chemistry-An Asian Journal*, vol. 11, no. 12, pp. 1804-1810, 2016.
- [156] Li, H., Liang, Y., Liu, Y., Liu, S., Li, P. and He, C., "Engineering doping level for enhanced thermoelectric performance of carbon nanotubes/polyaniline composites," *Composites Science and Technology*, vol. 210, p. 108797, 2021.
- [157] Li, H., Liu, S., Li, P., Yuan, D., Zhou, X., Sun, J., Lu, X. and He, C., "Interfacial control and carrier tuning of carbon nanotube/polyaniline composites for high thermoelectric performance," *Carbon*, vol. 136, pp. 292-298, 2018.
- [158] Li, H., Liu, Y., Li, P., Liu, S., Du, F. and He, C., "Enhanced Thermoelectric Performance of Carbon Nanotubes/Polyaniline Composites by Multiple Interface Engineering," *ACS Applied Materials & Interfaces*, vol. 13, no. 5, pp. 6650-6658, 2021.
- [159] Liu, S., Li, H. and He, C., "Simultaneous enhancement of electrical conductivity and seebeck coefficient in organic thermoelectric SWNT/PEDOT:PSS nanocomposites," *Carbon*, vol. 149, pp. 25-32, 2019.
- [160] Liu, S., Kong, J., Chen, H. and He, C., "Interfacial Energy Barrier Tuning for Enhanced Thermoelectric Performance of PEDOT Nanowire/SWNT/PEDOT:PSS Ternary Composites," *ACS Applied Energy Materials*, vol. 2, no. 12, pp. 8843-8850, 2019.
- [161] Mitra, M., Kargupta, K., Ganguly, S., Goswami, S. and Banerjee, D., "Facile synthesis and thermoelectric properties of aluminum doped zinc oxide/polyaniline (AZO/PANI) hybrid," *Synthetic Metals*, vol. 228, pp. 25-31, 2017.
- [162] Cho, C., Wallace, K.L., Tzeng, P., Hsu, J.H., Yu, C. and Grunlan, J.C., "Outstanding low temperature thermoelectric power factor from completely

- organic thin films enabled by multidimensional conjugated nanomaterials," *Advanced Energy Materials*, vol. 6, no. 7, p. 1502168, 2016.
- [163] Wu, Y., Farmer, D.B., Xia, F. and Avouris, P., "Graphene electronics: Materials, devices, and circuits," *Proceedings of the IEEE*, vol. 101, no. 7, pp. 1620-1637, 2013.
- [164] Wang, H., Hsu, A.L. and Palacios, T., "Graphene electronics for RF applications," in *2011 IEEE MTT-S International Microwave Symposium*, pp. 1-4, 2011.
- [165] Juntunen, T., Jussila, H., Ruoho, M., Liu, S., Hu, G., Albrow-Owen, T., Ng, L.W., Howe, R.C., Hasan, T., Sun, Z. and Tittonen, I., "Inkjet Printed Large-Area Flexible Few-Layer Graphene Thermoelectrics," *Advanced Functional Materials*, vol. 28, no. 22, p. 1800480, 2018.
- [166] Dey, A., Bajpai, O.P., Sikder, A.K., Chattopadhyay, S. and Khan, M.A.S., "Recent advances in CNT/graphene based thermoelectric polymer nanocomposite: A proficient move towards waste energy harvesting," *Renewable and Sustainable Energy Reviews*, vol. 53, pp. 653-671, 2016.
- [167] Zhang, Y., Zhang, Q. and Chen, G., "Carbon and carbon composites for thermoelectric applications," *Carbon Energy*, vol. 2, no. 3, pp. 408-436, 2020.
- [168] Wang, L., Yao, Q., Bi, H., Huang, F., Wang, Q. and Chen, L., "PANI/graphene nanocomposite films with high thermoelectric properties by enhanced molecular ordering," *Journal of Materials Chemistry A*, vol. 3, no. 13, pp. 7086-7092, 2015.
- [169] Hsieh, Y.Y., Zhang, Y., Zhang, L., Fang, Y., Kanakaraaj, S.N., Bahk, J.H. and Shanov, V., "High thermoelectric power-factor composites based on flexible three-dimensional graphene and polyaniline," *Nanoscale*, vol. 11, no. 14, pp. 6552-6560, 2019.
- [170] Wang, L., Bi, H., Yao, Q., Ren, D., Qu, S., Huang, F. and Chen, L., "Three-dimensional tubular graphene/polyaniline composites as high-performance elastic thermoelectrics," *Composites Science and Technology*, vol. 150, pp. 135-140, 2017.
- [171] Lin, Y.H., Lee, T.C., Hsiao, Y.S., Lin, W.K., Whang, W.T. and Chen, C.H., "Facile synthesis of diamino-modified graphene/polyaniline semi-interpenetrating networks with practical high thermoelectric performance," *ACS Applied Materials & Interfaces*, vol. 10, no. 5, pp. 4946-4952, 2018.

- [172] Park, C., Yoo, D., Im, S., Kim, S., Cho, W., Ryu, J. and Kim, J.H., "Large-scalable RTCVD Graphene/PEDOT:PSS hybrid conductive film for application in transparent and flexible thermoelectric nanogenerators," *RSC Advances*, vol. 7, no. 41, pp. 25237-25243, 2017.
- [173] Du, F.P., Cao, N.N., Zhang, Y.F., Fu, P., Wu, Y.G., Lin, Z.D., Shi, R., Amini, A. and Cheng, C., "PEDOT: PSS/graphene quantum dots films with enhanced thermoelectric properties via strong interfacial interaction and phase separation," *Scientific Reports*, vol. 8, 2018.
- [174] Wang, X., Meng, F., Wang, T., Li, C., Tang, H., Gao, Z., Li, S., Jiang, F. and Xu, J., "High performance of PEDOT:PSS/SiC-NWs hybrid thermoelectric thin film for energy harvesting," *Journal of Alloys and Compounds*, vol. 734, pp. 121-129, 2018/02/15/ 2018.
- [175] Kim, G.H., Shao, L., Zhang, K. and Pipe, K.P., "Engineered doping of organic semiconductors for enhanced thermoelectric efficiency," *Nature Materials*, vol. 12, no. 8, pp. 719-723, 2013.
- [176] Fan, Z., Du, D., Guan, X. and Ouyang, J., "Polymer films with ultrahigh thermoelectric properties arising from significant seebeck coefficient enhancement by ion accumulation on surface," *Nano Energy*, vol. 51, pp. 481-488, 2018.
- [177] Yemata, T.A., Zheng, Y., Kyaw, A.K.K., Wang, X., Song, J., Chin, W.S. and Xu, J., "Binary treatment of PEDOT:PSS films with nitric acid and imidazolium-based ionic liquids to improve the thermoelectric properties," *Materials Advances*, 2020.
- [178] Jiao, F., Di, C.A., Sun, Y., Sheng, P., Xu, W. and Zhu, D., "Inkjet-printed flexible organic thin-film thermoelectric devices based on *p*- and *n*-type poly (metal 1, 1, 2, 2-ethenetetrathiolate) s/polymer composites through ball-milling," *Philosophical Transactions of the Royal Society A: Mathematical, Physical and Engineering Sciences*, vol. 372, no. 2013, p. 20130008, 2014.
- [179] Cui, Y., Yan, J., Sun, Y., Zou, Y., Sun, Y., Xu, W. and Zhu, D., "Thermoelectric properties of metal-(Z)-1, 2-dihydroselenoethene-1, 2-dithiol coordination polymers," *Science Bulletin*, vol. 63, no. 13, pp. 814-816, 2018.
- [180] Huang, X., Qiu, Y., Wang, Y., Liu, L., Wu, X., Liang, Y., Cui, Y., Sun, Y., Zou, Y., Zhu, J. and Fang, W., "Highly Conducting Organic-Inorganic Hybrid Copper Sulfides $Cu_xC_6S_6$ ($x= 4$ or 5.5): Ligand-Based Oxidation-Induced

- Chemical and Electronic Structure Modulation," *Angewandte Chemie International Edition*, vol. 59, no. 50, pp. 22602-22609, 2020.
- [181] Nakashima, Y., Nakashima, N. and Fujigaya, T., "Development of air-stable n-type single-walled carbon nanotubes by doping with 2-(2-methoxyphenyl)-1, 3-dimethyl-2, 3-dihydro-1H-benzo [d] imidazole and their thermoelectric properties," *Synthetic Metals*, vol. 225, pp. 76-80, 2017.
- [182] Kim, D., Kim, Y., Choi, K., Grunlan, J.C. and Yu, C., "Improved thermoelectric behavior of nanotube-filled polymer composites with poly (3, 4-ethylenedioxythiophene) poly (styrenesulfonate)," *ACS Nano*, vol. 4, no. 1, pp. 513-523, 2010.
- [183] Moriarty, G.P., De, S., King, P.J., Khan, U., Via, M., King, J.A., "Thermoelectric behavior of organic thin film nanocomposites," *Journal of Polymer Science Part B: Polymer Physics*, vol. 51, no. 2, pp. 119-123, 2013.
- [184] Zhu, Z., Wang, L. and Gao, C., "Thermoelectric properties of PEDOTs," in *Advanced PEDOT Thermoelectric Materials*: Elsevier, 2022, pp. 73-95.
- [185] Yemata, T.A., Zheng, Y., Kyaw, A.K.K., Wang, X., Song, J., Chin, W.S. and Xu, J., "Binary treatment of PEDOT: PSS films with nitric acid and imidazolium-based ionic liquids to improve the thermoelectric properties," *Materials Advances*, vol. 1, no. 9, pp. 3233-3242, 2020.
- [186] Hayashi, D., Ueda, T., Nakai, Y., Kyakuno, H., Miyata, Y., Yamamoto, T., Saito, T., Hata, K. and Maniwa, Y., "Thermoelectric properties of single-wall carbon nanotube films: effects of diameter and wet environment," *Applied Physics Express*, vol. 9, no. 2, p. 025102, 2016.
- [187] Kim, S., Mo, J.H. and Jang, K.S., "Solution-processed carbon nanotube buckypapers for foldable thermoelectric generators," *ACS Applied Materials & Interfaces*, vol. 11, no. 39, pp. 35675-35682, 2019.
- [188] Mo, J.H., Kim, J.Y., Kang, Y.H., Cho, S.Y. and Jang, K.S, "Carbon nanotube/cellulose acetate thermoelectric papers," *ACS Sustainable Chemistry & Engineering*, vol. 6, no. 12, pp. 15970-15975, 2018.
- [189] Selvan, K.V., Hasan, M.N. and Mohamed Ali, M.S., "State-of-the-art reviews and analyses of emerging research findings and achievements of thermoelectric materials over the past years," *Journal of Electronic Materials*, vol. 48, no. 2, pp. 745-777, 2019.

- [190] Jin Bae, E., Hun Kang, Y., Jang, K.S. and Yun Cho, S., "Enhancement of thermoelectric properties of PEDOT: and tellurium-PEDOT:PSS hybrid composites by simple chemical treatment," *Scientific Reports*, vol. 6, no. 1, pp. 1-10, 2016.
- [191] Elmoughni, H.M., Menon, A.K., Wolfe, R.M. and Yee, S.K., "A textile-integrated polymer thermoelectric generator for body heat harvesting," *Advanced Materials Technologies*, vol. 4, no. 7, p. 1800708, 2019.
- [192] Wen, N., Fan, Z., Yang, S., Zhao, Y., Li, C., Cong, T., Huang, H., Zhang, J., Guan, X. and Pan, L., "High-performance stretchable thermoelectric fibers for wearable electronics," *Chemical Engineering Journal*, vol. 426, p. 130816, 2021.
- [193] Hyland, M., Hunter, H., Liu, J., Veety, E. and Vashaee, D., "Wearable thermoelectric generators for human body heat harvesting," *Applied Energy*, vol. 182, pp. 518-524, 2016.
- [194] Fan, Z., Li, P., Du, D. and Ouyang, J., "Significantly enhanced thermoelectric properties of PEDOT: PSS films through sequential post-treatments with common acids and bases," *Advanced Energy Materials*, vol. 7, no. 8, p. 1602116, 2017.

LIST OF PUBLICATIONS

Indexed Journals

1. **M. N. Hasan**, M. Nafea, N. Nayan, and M. S. Mohamed Ali, "Thermoelectric Generator: Materials and Applications in Wearable Health Monitoring Sensors and Internet of Things Devices," *Advanced Materials Technologies*, p. 2101203, 2021. (**Q1, IF: 8.856**) (Part of Chapter 2)
2. **M. N. Hasan** and M. S. Mohamed Ali, "Influence of leg geometry on the performance of Bismuth Telluride-based Thermoelectric Generator," *ELEKTRIKA-Journal of Electrical Engineering*, 20(2-2), 25-29. (**Scopus Indexed**) (Part of Chapter 4 and Chapter 5)
3. **M. N. Hasan**, S. Sahlan, K. Osman, and M. S. Mohamed Ali, "Energy harvesters for wearable electronics and biomedical devices," *Advanced Materials Technologies*, vol. 6, no. 3, p. 2000771, 2021. (**Q1, IF: 8.856**) (Part of Chapter 2)
4. **M. N. Hasan**, H. A. Rahim, M. A. Ahmad, and M. S. M. Ali, "Modelling and simulation of magnesium antimonide based thermoelectric generator," *Indonesian Journal of Electrical Engineering and Computer Science*, vol. 19, no. 2, pp. 686-692, 2020. (**Scopus Indexed**) (Part of Chapter 3 and Chapter 4)
5. **M. N. Hasan**, H. Wahid, N. Nayan, and M. S. Mohamed Ali, "Inorganic thermoelectric materials: A review," *International Journal of Energy Research*, vol. 44, no. 8, pp. 6170-6222, 2020. (**Q1, IF: 4.672**) (Part of Chapter 2)
6. K. V. Selvan, **M. N. Hasan**, and M. S. Mohamed Ali, "Methodological reviews and analyses on the emerging research trends and progresses of thermoelectric generators," *International Journal of Energy Research*, vol. 43, no. 1, pp. 113-140, 2019. (**Q1, IF: 4.672**) (Part of Chapter 2)

7. K. V. Selvan, **M. N. Hasan**, and M. S. Mohamed Ali, "State-of-the-art reviews and analyses of emerging research findings and achievements of thermoelectric materials over the past years," *Journal of Electronic Materials*, vol. 48, p. 745-777, 2019. (**Q3, IF: 2.047**) (Part of Chapter 2)
8. **M. N. Hasan**, N. Nayan, M. Nafea, A. G. Muthalif, and M. S. Mohamed Ali, "Novel structural design of wearable thermoelectric generator with vertically oriented thermoelements," *Energy*, vol. 259, p. 125032, 2022. (**Q1, IF: 8.857**) (Part of Chapter 4)
9. **M. N. Hasan**, M. I. A. Asri, T. Saleh, A. G. Muthalif, and M. S. Mohamed Ali, "Wearable Thermoelectric Generator with Vertically Aligned PEDOT:PSS And Carbon Nanotubes Thermoelements for Energy Harvesting," *International Journal of Energy Research*, 2022. <https://doi.org/10.1002/er.8283> (**Q1, IF: 4.672**) (Part of Chapter 5)

Indexed Conference Proceedings

1. **M. N. Hasan**, Y. M. Yunos, and M. S. M. Ali, "Structural Optimization of a Bismuth Telluride-Based Thermoelectric Generator Using Finite Element Analysis," in *2021 IEEE International Power and Renewable Energy Conference (IPRECON)*, 2021: IEEE, pp. 1-4. (Part of Chapter 3 and Chapter 4)
2. **M. N. Hasan**, M. Y. B. Hashem, M. A. Siddique, M. A. M. Yunus, and M. S. M. Ali, "Finite Element Analysis of Thermoelectric Power Generation from Human Wrist," in *2021 IEEE Symposium on Industrial Electronics & Applications (ISIEA)*, 2021: IEEE, pp. 1-5. (Part of Chapter 4 and Chapter 5)
3. **M. N. Hasan** and M. S. Mohamed Ali, "Optimal Design of Thermoelectric Generator with Vertically Aligned PEDOT:PSS Thermoelements," *AIP Conference Proceedings*, 2022. **Accepted** (Part of Chapter 4)